Multiple Region Reverse Frequency Allocation Scheme in Downlink Heterogeneous Networks

By

Rehan Zahid

2012-NUST-MS-EE(S)-60880

Supervisor

Dr. Syed Ali Hassan

Department of Electrical Engineering

A thesis submitted in partial fulfillment of the requirements for the degree of Masters in Electrical Engineering (MS EE-TCN)

In

School of Electrical Engineering and Computer Science,

National University of Sciences and Technology (NUST),

Islamabad, Pakistan.

(Oct 2014)

Approval

It is certified that the contents and form of the thesis entitled "**Multiple Region Reverse Frequency Allocation Scheme in Downlink Heterogeneous Networks**" submitted by **Rehan Zahid** have been found satisfactory for the requirement of the degree.

Advisor: **Dr. Syed Ali Hassan**

Signature: _____

Date: _____

Committee Member 1: **Dr. Adnan Khalid Kiani**

Signature: _____

Date: _____

Committee Member 2: **Dr. Hassaan Khaliq**

Signature: _____

Date: _____

Committee Member 3: **Mr. Khurram Shahzad**

Signature: _____

Date: _____

Dedication

I dedicate this thesis to my parents, teachers and brothers who helped me throughout my research phase.

Certificate of Originality

I hereby declare that this submission is my own work and to the best of my knowledge it contains no materials previously published or written by another person, nor material which to a substantial extent has been accepted for the award of any degree or diploma at National University of Sciences & Technology (NUST) School of Electrical Engineering & Computer Science (SEECS) or at any other educational institute, except where due acknowledgement has been made in the thesis. Any contribution made to the research by others, with whom I have worked at NUST SEECS or elsewhere, is explicitly acknowledged in the thesis.

I also declare that the intellectual content of this thesis is the product of my own work, except for the assistance from others in the project's design and conception or in style, presentation and linguistics which has been acknowledged.

Author Name: **Rehan Zahid**

Signature: _____

Acknowledgment

I am very thankful to Almighty Allah who gave me strength and support throughout the research work. It would not have been possible without His blessings.

I am eternally grateful to my family who have always supported me by their encouragement and by moral and emotional support throughout the dissertation. This thesis is a milestone in my academic carrier. Extensive research has increased my knowledge in learning theories and concepts.

My utmost gratitude to Dr. Syed Ali Hassan, who provided me assistance and valuable thoughts in my research work. His recommendations and advices have enabled me to fulfill the requirements of the dissertation effectively. He has been a great source of inspiration for me and his immense knowledge and commitment helped me to accomplish my task in an effective manner.

My special thanks to my committee members, Dr. Hassaan Khaliq, Dr. Adnan Khalid Kiani, Mr. Khurram Shahzad and to all those friends and teachers who contributed towards the successful completion of my dissertation.

Rehan Zahid

Table of Contents

1 Introduction **1**

1.1 What are Femtocells 4

1.2 Technical Aspects of Femtocells 6

1.2.1 2G Femtocells 7

1.2.2 3G Femtocells 8

1.2.3 OFDMA-based Femtocells 9

1.3 Advantages of Femtocells 9

1.4 Disadvantages of Femtocells 10

1.5 Issues related to the deployment of Femtocell technology . . . 11

1.5.1 Access Modes 11

1.5.2 Mobility Management and Handovers 12

1.5.3 Femtocell Deployment Issues 13

1.5.4 Interference Management 13

1.6 Research Gap and Problem Statement 13

1.6.1 Problem Statement 14

1.7 Thesis Contribution 14

1.8 Thesis Organization 15

1.8.1 Chapter 2 15

1.8.2 Chapter 3 16
1.8.3 Chapter 4 16
1.8.4 Chapter 5 16
1.8.5 Chapter 6 16
1.8.6 Chapter 7 17

2 Interference Issues due to Femtocell Deployment 18

2.1 Introduction 18
2.2 Co-tier Interference 19
2.3 Cross-tier Interference 20
2.4 Interference Management Methods 22

3 Background and Literature Review 24

3.1 Introduction 24
3.2 Fractional Frequency Reuse (FFR) 24
3.3 Soft Fractional Frequency Reuse (SFFR) 25
3.4 Power Control Algorithm 26
3.5 Subchannel Allocation 27
3.6 Dynamic Frequency Reuse 28
3.7 Static Frequency Band Allocation 28
3.8 Shared Frequency Band Allocation 29
3.9 Subset Frequency Band Allocation 29
3.10 Reverse Frequency Allocation Scheme 30

4 System Architecture 33

4.1 Introduction 33
4.2 Interference Modeling and Region Selection 36

4.2.1 Optimal Partitioning of Regions 37

5 Stochastic Modeling of Multiple Region RFA 40

5.1 Introduction 40

5.2 Stochastic Modelling of the Network 43

6 Simulation Results and Performance Analysis 50

6.1 Introduction 50

6.2 Numerical results and performance analysis 55

7 Conclusion and Future Work 61

7.1 Conclusion 61

7.2 Future Work 62

List of Figures

1.1 User equipment connection to core network [14] 5

1.2 Typical indoor femtocell structure [14] 5

1.3 Types of femtocells [14] 8

2.1 Types of interference in two tier networks [14] 19

2.2 Uplink and downlink co-tier interference in two tier networks [14] 20

2.3 Uplink and downlink cross-tier interference in two tier networks [14] 21

3.1 Fractional frequency reuse (FFR) [29] 25

3.2 Soft fractional frequency reuse (SFFR) [30] 26

3.3 Downlink power control scheme [31] 27

3.4 Frequency allocation using dedicated frequency band scheme [33] 28

3.5 Frequency allocation using shared frequency band scheme [33] 29

3.6 Frequency allocation using subset frequency band scheme [33] 30

4.1 Reverse frequency allocation of 4 regions. 34

4.2 Frequency distribution for 4 regions. 34

4.3 Worst-case scenario in 4-region RFA. The direction of arrows shows the interference direction. 38

5.1 2-RFA interfering scenarios; only downlink FUEs scenarios are shown. 41

5.2 4-RFA geometry of 2-tier Hetnet; only first scenario is shown. 44

6.1 Average system outage probability of 2 region RFA. 51

6.2 Average system outage probability of 4 region RFA. 51

6.3 Average system outage probability at different cell radius. . . . 53

6.4 Average system outage probability at different users and cell radius. 54

6.5 Average coverage probability of FUE at different density of FAPs (λ_2); ($\lambda_1 = 200$, $\tau = -6.98dB$) 56

6.6 Average coverage probability of FUE at different density of MUEs (λ_1); ($\lambda_2 = 1600, \tau = -6.98dB$) 57

6.7 Average coverage probability of FUE at different SIR threshold (τ); ($\lambda_1 = 200, \lambda_2 = 1600$) 58

6.8 Average coverage probability of FUE at different cell radius; ($\lambda_1 = 200, \lambda_2 = 1600, \tau = -6.98dB$) 59

List of Tables

1.1 FAP and Wi-Fi specifications [14] 7

2.1 Types of interference in two tier networks 22

5.1 4-RFA interference scenarios 43

6.1 Simulation Parameters 52

List of Abbreviations

Abbreveation	Description
MBS	Macrocell Base Station
FAP	Femtocell Access Point
FUE	Femtocell User Equipment
MUE	Macrocell User Equipment
RFA	Reverse Frequency Allocation
SINR	Signal-to-Interference Plus Noise Ratio
PPP	Poisson Point Process
HCNs	Heterogeneous Cellular Networks
WCNs	Wireless Cellular Networks

Abstract

Femtocell access points (FAPs) are low-powered and small-sized base stations that provide high data rates and coverage to the indoor users. Because of their operation in the same spectrum as that of macrocells, interference becomes a major problem. In this thesis, we study the downlink performance of a heterogeneous cellular network (HCN) by proposing a Reverse frequency allocation (RFA) scheme that divides the cell service area into multiple regions and assign frequencies to various cell entities in such a way that the major interference is avoided without disturbing the overall spectral efficiency. Moreover, we provide a multiple region 2-tier downlink model using RFA scheme. We derive a closed-form expression for the coverage probability of femtocell user equipment (FUE) using different RFA schemes under open access mode. Where FAPs and MUEs are modeled as independent Poisson point process (PPP). Using simulations, we show that for reasonable values of signal-to-interference ratio (SIR), multiple regions enhance the coverage probability of an FUE. It is shown that a 4-region RFA outperforms the other RFA schemes at different densities of FAPs and MUEs as well as for different values of threshold for the same set of parameters.

Chapter 1

Introduction

The rapid increase in the proliferation of wireless devices has increased the requirements of capacity. In this modern era, more and more users prefer the wireless networks as compared to the wired technology. Wireless networks mainly comprises two technologies, the wireless cellular networks (WCNs), which provide the voice communication to users having high mobility and wireless local area networks (WLANs) that enable the communication to users with high data rates but with limited mobility. To fulfill the demand of users toward wireless technology, wireless networks needs to provide more data rates and services as wired networks. A study in [1] estimates that about 39 fold increase in data services from 2009 to 2014. On the other hand, wireless cellular networks replace the wired networks by providing high data rates and coverage [2]. The standards like 3GPPs High Speed Packet Access (HSPA), Long Term Evolution (LTE), LTE advanced, Ultra Wide Band (UWB) and Worldwide Interoperability for Microwave Access (WiMAX) have been developed to offer high data rates and services to their end users [3].

The fundamental approach to achieve high data rates is that the signal-to-interference plus noise ratio (SINR) must be greater than a pre-defined threshold by keeping one thing in mind that the transmitter should not create a significant interference to the other receivers by transmitting high power signals. This phenomenon leads toward the fact that the distance between the transmitter and receiver should be reduced so that the end user can receive a signal with higher SINR.

Capacity can also be increased with the provision of large number of channels per cell. On the other hand, it can also be increased by reducing the number of cells in a given cluster so that channels can be reused more and more efficiently in the nearby cluster. Cell sectoring and cell splitting are widely used to increase the capacity in current wireless technologies. In addition by reducing the number of cells in a cluster, distance to other cells using the same channel is reduced that leads toward the interference. Various interference mitigation and interference avoidance schemes are used to avoid this type of interference.

In an outdoor environment, users normally receive the signal with higher SINR but this becomes a challenging task to provied the higher signal strength to the users in an indoor environment. The ABI research mention that, more than 70% of data traffic and more than 50% of voice services are expected to generate from indoor users [4]. Another survey shows that almost 45% household and 30% business users are not satisfied with their indoor coverage [5]. The indoor users require high power signals from the serving base station (BS) due to the high penetration losses, which means that the power to the other users would be reduced from the base station that leads to-

ward the reduced throughput. On the other hand, to fulfill the demand of users by increasing number of base stations is also very expensive in term of cost, planning and optimization as well. Moreover, coding and modulation schemes used in LTE, LTE advanced and WiMAX require better condition of channel, this means that the Quality-of-Service (QoS) is not guaranteed in case of indoor coverage due to the channel variation [6].

Picocells, relays or repeaters and distributed antenna systems (DAS) provide the solution of indoor coverage to the indoor users. Picocells perform in the same way as that of macrocells, which are connected with each other as well as with the macrocells through cables. The distributed antenna systems consists of several distributed antenna elements and home base station. Using optical fibers or RF links, these antenna elements are connected to the home base station. They provide the good coverage to the users where the macrocell base station (MBS) signals cannot reach. DAS can also decrease its transmit power, which leads toward the reduction in the interference and increase in capacity as well. Antenna elements are spread over the desired area, consist of transceivers, which send information back to the base station (BS) where further processing is done [7]. Although both picocells and DAS provides the cost effective solution as compared to macrocell base staions but their deployment is still expensive in small offices and homes.

Another emerging topic is relaying in LTE for indoor coverage [8]. This technique requires the relay to provide high data rates to the indoor users. To provide high data rates and services, relay is usually placed inside the buildings and homes to compensate the penetration losses occurs due to walls of buildings. There are two types in which relaying are performed. One

is Amplify and Forward Relaying (AF) while the second one is Decode and Forward Relaying (DF) [8][9]. In first mode, the relay receives signal, amplify it and retransmit again. In this case the noise is also amplify in the same proportion as the data signal, which reduce the overall capacity of the system. While in the second mode, relay receives a signal, decode and demodulates before the retransmission of the signal. This results the decrement in the noise level. So DF relaying has more advantages as compared to AF relaying [10].

Due to increasing demand of wireless services, there is a significant potential for using a new technology named as femtocells [11]-[13]. Femtocells are also called home base station looks like a wireless router. The home access points provide the indoor coverage, installed by user that connects the user equipment (UE) to cellular core network via subscriber broadband Internet access. Access point also known as femtocell access point (FAP) provides high quality voice, data and multimedia services to its intended users. Femtocells provide good coverage as compared to DAS and picocells but also suffer many challenges. They require either the separate portion of spectrum or the same portion of the spectrum that is utilized by the macrocell. When femtocell uses the same spectrum as that of macrocell, interference becomes a major problem between the neighboring femtocells or between the femtocells to macrocells.

1.1 What are Femtocells

The femtocell base station is also known as femtocell access point (FAP), which is installed by the users in their premises. FAP is usually connected to

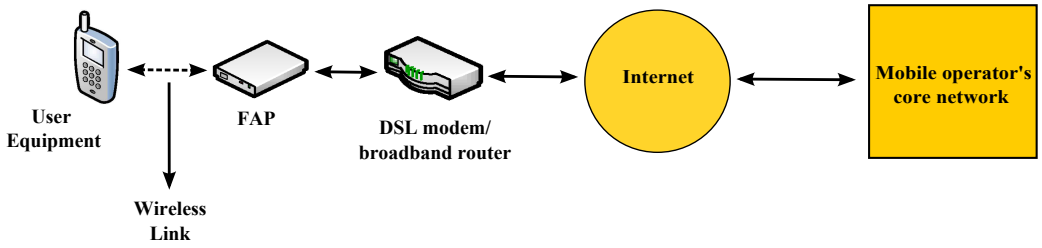

Figure 1.1: User equipment connection to core network [14]

operator's core network through user's DSL connection as shown in Figure 1.1. The typical indoor femtocell structure where multiple indoor users are connected to FAP and finally with operator core network is shown in Figure 1.2.

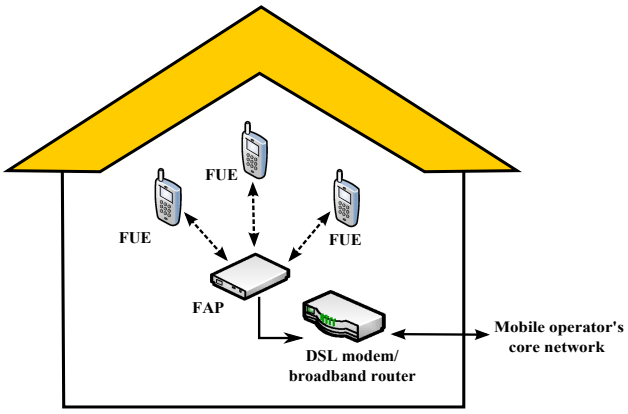

Figure 1.2: Typical indoor femtocell structure [14]

Femtocells are usually called Home Node B (HNB) in WCDMA systems and Home e Node B (H(e)NB) in LTE systems. The most important function in 3GPP release 8 is Closed Subscriber Group known as CSG. In closed access mode only registered user equipments can connected to the FAP while the other users are rejected that are not registered to that FAP. This mode is enhanced in release 9 gives open access mode and hybrid access mode.

1.2 Technical Aspects of Femtocells

Femtocells provide the better indoor coverage due to small radius usually in the order of 10-50m. As the distance between transmitter and receiver decreases, the transmitted signal will experience a less attenuation and receiver receives a better signal strength. The quality of received signal is usually measured in term of SINR. SINR is the function of signal power from serving base station, signal power from interfering base stations, pathlosses, shadowing and fading. The penetration losses due to walls also degrade the interfering signals that are more prominent at higher frequencies. Moreover femtocells provide the coverage to small number of users as compared to macrocells, so it can provide the large portion of resources to its users that yields a good quality-of-service. Femtocells are usually deployed in two modes.

1) Co-channel deployment
2) Separate channel deployment

In first mode, femtocells utilize the same spectrum as that of macrocells while in second mode femtocells utilize the separate portion of spectrum to avoid the interference between femtocell to macrocell. Operators usually prefer the co-channel deployment because separate channel deployment is not a efficient utilization of resources. In case of co-channel deployment, interference will be high because both the femtocells and macrocells are utilizing the same portion of the spectrum. So there is a need of efficient interference management techniques to avoid this interference. Femtocells also provide

Table 1.1: FAP and Wi-Fi specifications [14]

Specifications	**3G Femtocell (HSPA)**	**Wi-Fi**
Data rates	7.2-14.4Mbps	11 and 54Mbps
Operational Frequency	1.9-2.6GHz	2.4-5GHz
Power	10-100mW	100-200mW
Range	10-30m	100-200m
Services	Primarily voice and data	Primarily data and voice

the coverage to macrocell user equipments (MUEs) at the edge of the cell, where the MUEs do not receive high quality signals from the macrocell base station (MBS).

Both Wi-Fi and FAP have similarities but the difference as well. Similarities in term of internet as backhaul connection while the difference in term of technology which they implement. FAP provides voice, data as well as multimedia services while Wi-Fi and WLANs provides mainly data services [15]. Table 1.1 shows the main differences between Wi-Fi and FAP. There are different types of femtocells which provide different services based on technology of air interface.

1.2.1 2G Femtocells

2G femtocells typically based on GSM air interface technology. GSM has large number of users around the world. Provision of 3G services and femtocells are not possible with GSM technology. The 2G femtocells offer low cost as compared to new versions [16]. The main drawback of GSM femtocells is that they use GPRS for data services which does not provide high data

rates to the end users. Moreover GSM femtocells do not provide good power control schemes to mitigate the interference that arises due to co-channel deployment of femtocells. But deployment of 2G femtocells is feasible in developing countries where cellular networks are basically used for voice services only [17]. The main types of femtocells are shown in Figure 1.3.

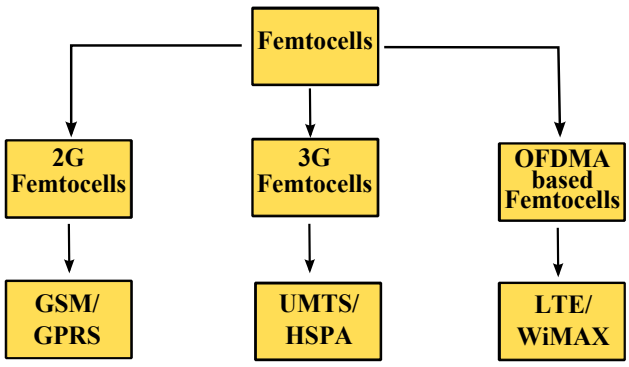

Figure 1.3: Types of femtocells [14]

1.2.2 3G Femtocells

The 3G femtocells typically based on universal mobile telecommunication systems (UMTS). They provide high data rates as compared to 2G femtocells. They also provide the better power allocation to mitigate the interference between the femtocells as compared to 2G femtocells. They are standardized by 3GPP as HNBs [18]. They also have a potential of connecting through IP based networks that make it more applicable to heterogeneous cellular networks.

1.2.3 OFDMA-based Femtocells

LTE and WiMAX femtocells use orthogonal frequency division multiplexing (OFDM) as their physical layer technology. They have good reputation in term of high data rates and services and considered to be the future of indoor technology. A lot of research is going on efficient implementation of such OFDMA-based femtocells.

1.3 Advantages of Femtocells

The fundamental advantage of the femtocells is to provide the coverage in the areas where the MBS have weak signal strength. i.e., inside the buildings, homes, offices or usually at the edge of the cellular area. The some other advantages are mentioned below:

1) Femtocell enables the communication with high data rates and good quality of service to indoor users by offloading the data traffic from the main macro base station (MBS), which is an expensive radio resource.

2) Femtocell is a low-powered, and small-sized base station with less complexity that provides high data rates and improves the quality of service to the indoor users.

3) It is very expensive to deploy a large number of MBS in order to provide the good coverage and to meet the increasing demand of the high capacity networks. This problem is overcome by using the femtocell technology.

4) Femtocells can also operate in closed access mode in which the specific users can access the services of the femtocell. It is decided by the owner of the femtocell.

5) Usually the cell towers are back-hauled with cables having bandwidth around 2Mbps that may not be suitable for 3G and 4G services and require the sufficient upgradation. In case of femtocells, they are connected to opertor's core network through DSL broadabnd internet connection and having no upgradation issues.

1.4 Disadvantages of Femtocells

The disadvantages of the femtocells are following:

1) Due to homogeneous deployment of femtocells in macro-cellular network area, interference is one of the main problem due to the same spectrum utilized by the femtocellular and overlaid macro-cellular network.

2) For call and data transfer services, femtocells use the intenet connection, which leads toward the poor call quality if the large data files are downloaded from the internet at the same time.

3) In case of closed access mode, the interference will be high because the FUE will remain connected to its intended FAP even it is receiving the stronger signal from the neighboring FAP.

4) As the FUE is connected to the operators core network through internet connection so there must be a stable internet connection to provide the good quality-of-service without any delay. Moreover, the efficient mechanism is required to prioritize the femtocell traffic.

1.5 Issues related to the deployment of Femtocell technology

As the femtocell is very promising technology to provide high data rates and coverage to the users in an indoor environment but on the other side there are many issues related to the deployment of femtocells that are mentioned below:

1.5.1 Access Modes

The femtocell can support the limited number of users so it must be clear that to which user it will privide the services. Currently there are three access modes which have been defined for the femtocells [19].

1) Open access mode: In this mode every user can use the femtocell services and get benefits from it.

2) Closed access mode: In this mode only registered users can access the femtocell. The users who are not registered would be regected. The owner decides that which user can access the femtocell. It is referred to as closed subscriber group (CSG) by 3GPP release 9.

3) Hybrid access mode: In this mode only specific number of outside users can access the femtocell. This access of outside users is defined by the each operator separately.

The open access mode is not mostly used because the owner who pay charges for the FAP, backhaul connection and electricity does not want that everyone use his FAP's resources. It is mostly used in public place like shop-

ping malls, air ports and terminals etc. Users of home and offices generally use the close access mode, but the major drawback of this mode is that any other subscriber would not get access to FAP even it is very close to that FAP. So it causes the significant interference to those FAP users. These access modes are very important and have direct impact on the interference. Hybrid access mode is also a good choice but in this case, allowing a large number of outside users would have a negative impact on the registered users [20][21].

1.5.2 Mobility Management and Handovers

In case of dense deployment of femtocells, it is the key challenge to manage the mobility and handovers. There is large number of neighboring femtocells distributed in an ad-hoc manner so it is difficult to keep track of neighbors constantly. The interaction with other femtocells to manage the handover and mobility is also difficult in case of limited resources. To solve this problem, a scheme is purposed in which intermediate node is introduced that manage the handovers [22]. Access modes have great impact on handovers. In open access mode, there are large numbers of handovers which is reduceed in closed access mode and hybrid access mode. There are different algorithms for different schemes that have been developed to manage the handovers. Some algorithm takes into account of speed of UE and signal strength, while the other takes into account of QoS and velocity of UE.

1.5.3 Femtocell Deployment Issues

The co-channel deployment and the separate channel deployment of femtocells has its own advantages and disadvantages. In separate channel deployment, both femtocells and macrocells operate in their dedicated spectrum so there will be no interference between the femtocells and macrocells. In this case the spectral efficiency will be compromised. In co-channel deployment both femtocells and macrocells share the available spectrum that leads toward the efficient utilization of resources but in this case the interference will be high. Hence there must be a mechanism that the operators reuse the spectrum more and more in order to meet the increasing demand of the network and to reduce the interference to a significant level as well.

1.5.4 Interference Management

Interference management is one of the key challenges when femtocells are deployed in an ad-hoc manner. Operators usually prefer the co-channel deployment of femtocells in which they use the same portion of spectrum as the macrocells in order to meet the increasing demand of the network. Due to the utilization of same spectrum as that of macrocells, interference becomes a major problem. So there must be a interference avoidance scheme that can reduce the interference to a significant level.

1.6 Research Gap and Problem Statement

A lot of research work has been done to overcome the problem of interference that arises due to the co-channel deployment of femtocells within

the macrocell network area. The research work mainly consists of many frequency allocation schemes such as dedicated frequency band allocation schemes, shared frequency band allocation schemes, subset frequency band allocation, soft frequency reuse (SFR), fractional frequency reuse (FFR) and optimised fractional frequency reuse (OFFR). All the schemes has its own advantages and disadvantages in term of interference and the spectral efficiency. In this thesis, we have proposed a reverse frequency allocation scheme (RFA) for downlink scenarios, by dividing the cell service area into multiple regions and assign frequencies to various cell entities in such a way that the major interference is avoided. RFA scheme not only improves the spectral efficiency by utilizing the complete spectrum within one cell but also eliminates the strong interference due to macrocell base station on the femtocell users.

1.6.1 Problem Statement

"The objective of this thesis is to provide a frequency allocation scheme, which minimize the downlink co-tier and cross-tier interferences to significant level and to provide some closed form mathematical expressions that capture the important metrics like SINR, coverage probability and average rates"

1.7 Thesis Contribution

The contribution of this thesis is that we study the downlink performance of a heterogeneous network by proposing a Reverse frequency allocation (RFA) scheme by dividing the cell service area into multiple regions and assign

frequencies to various cell entities in such a way that the major interference is avoided. We analyze and evaluate the achievable performance of this technique for the downlink scenario. Using simulations, we show that under reasonable signal-to-interference plus noise ratio (SINR) values, multiple regions enhance the performance of users by decreasing the overall system outage probability. It is shown that a 4-region RFA scheme provides almost double performance gain over a 2-region RFA scheme for the same set of parameters. Moreover, we provide a multiple region 2-tier downlink model using RFA scheme. We derive a closed-form expression for the coverage probability of femtocell user equipment (FUE) using different RFA schemes under open access mode. Where FAPs and MUEs are modeled as independent Poisson point process (PPP). Using simulations, we show that for reasonable values of signal-to-interference ratio, multiple regions enhance the coverage probability of an FUE. It is shown that a 4-region RFA outperforms the other RFA schemes at different densities of FAPs and MUEs as well as for different values of threshold for the same set of parameters.

1.8 Thesis Organization

The rest of the thesis is organized as follows.

1.8.1 Chapter 2

Chapter 2 describes the interference issues related to the femtocell deployment that arises due to the co-channel deployment of femtocell within the area of macrocells.

1.8.2 Chapter 3

chapter 3 desribes the related work and literature review. In this chapter, different frequency allocation schemes proposed by the researchers for interference management are discussed. Detailed analysis of each scheme has been done and thier weak points have been pointed out.

1.8.3 Chapter 4

In chapter 4, the system architecture which is used to implement the Reverse frequency allocation (RFA) scheme in a single cell downlink heterogeneous networks has been discussed in detail.

1.8.4 Chapter 5

In chapter 5, stochastic geometry-based analysis of multiple region reverse frequency allocation scheme in downlink HetNets has been discussed. Moreover, multiple region 2-tier downlink model using RFA scheme has been presented in which a closed-form expression for the coverage probability of femtocell user equipment (FUE) using different RFA schemes under open access mode has been provided.

1.8.5 Chapter 6

In chapter 6, performance analysis and simulation results of proposed RFA scheme and its comparison with other RFA schemes has been disscused in detail.

1.8.6 Chapter 7

Chapter 7 contains the conclusion and the proposed future work.

Chapter 2

Interference Issues due to Femtocell Deployment

2.1 Introduction

The co-channel deployment of femtocells within the overlaid macrocells creats a significant interference due to the utilization of same resources as that of macrocells. Due to homogeneous deployment of femtocells, cellular architecture changes and now consists of two tiers. First tier is the conventional macrocell network while the 2nd tier is known as femtocell network. The interference in two tier network mainly consists of two types as shown in Figure 2.1.

1) Co-tier interference
2) Cross-tier interference

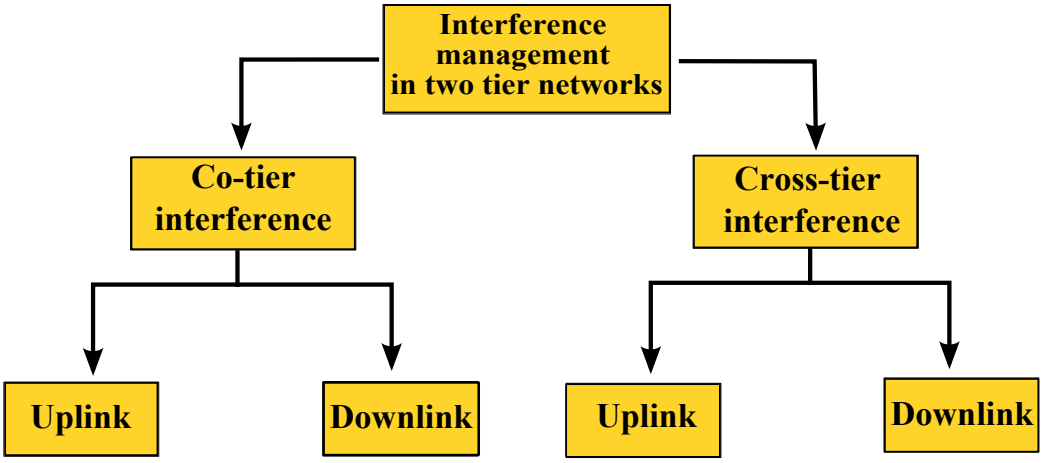

Figure 2.1: Types of interference in two tier networks [14]

2.2 Co-tier Interference

Co-tier inteference occurs due to the network elements that belongs to the same layer or tier of the network. i.e., from one femtocell to the neighboring femtocell. Femtocells are deployed randomly and their separation is not enough to avoid the interference. The overall interference at a certain FAP, from the neighboring femtocells must be less than a certain threshold in order to establish a communication link otherwise victim FAP would be in dead zone and link could not be established. Threshold level of SINR depends upon the air interface technology and different for different QoS [23]. Co-tier interference would be large in case of close access mode as compared to the open access and hybrid access mode [24]. So the dead zone would be larger for closed access as compared to others modes.

The uplink co-tier interference occurs due to femtocell user equipment (FUE). As the separation among the femtocells are not enough so the FUE of neighboring femtocells is the source of interference. If FUE of neighboring

femtocell is transmitting at higher power then its signals also approaches to the nearer FAP that introduce the interference to that FAP. This scenario is also shown in Figure 2.2.

The downlink co-tier interference occurs due to the FAP. When a FAP give a service to its users, the FUEs of nearby femtocells also receive that signal which basically leaks through windows or doors of the serving femtocell. So the victim FUEs experience interference. It is shown in Figure 2.2.

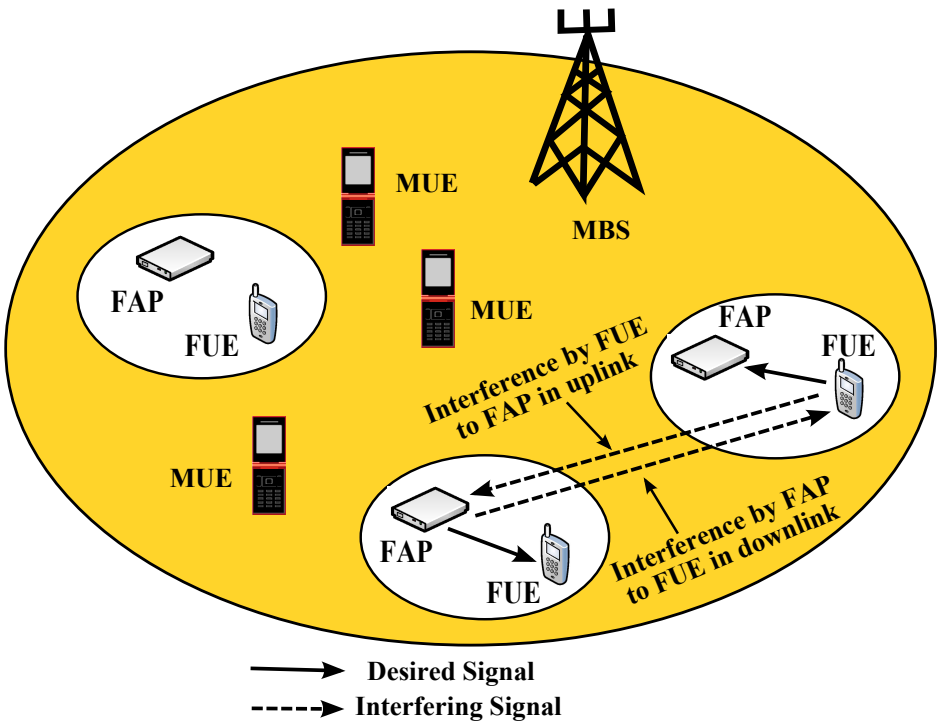

Figure 2.2: Uplink and downlink co-tier interference in two tier networks [14]

2.3 Cross-tier Interference

This type of interference occurs due to the network elements that belongs to the different layer or tier of the network. i.e., from femtocell to macrocell. For

example, when FAP sends a signal to its users, the MUE nearby to that FAP also receives a signal that experiences a significant interference. Similarly, MUE also cause a interference to nearer FAP during uplink operation.

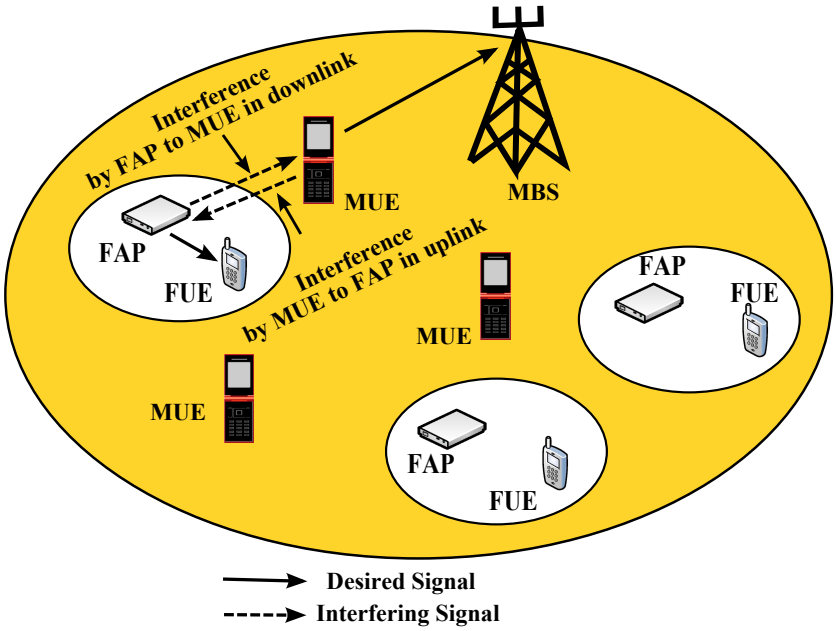

Figure 2.3: Uplink and downlink cross-tier interference in two tier networks [14]

Uplink cross tier interference also occurs, when FUE transmit at higher power near the MBS. In a similar way, when MUE transmit at higher power near the FAP. Similarly, there are two scenarios for downlink interference. First is, when FAP is transmitting and nearby MUE also receives its signal and other case is when MBS is transmitting and FUE also receives its signal. The uplink and downlink interfering scenarios are shown in Figure 2.3. In summary, the complete interfering scenarios are shown in Table. 2.1.

Table 2.1: Types of interference in two tier networks

Sr. No	Aggressor	Victim	Type of interference	Mode of transmission
1	MUE	FBS	Cross-tier	Uplink
2	MBS	FUE	Cross-tier	Downlink
3	FUE	MBS	Cross-tier	Uplink
4	FBS	MUE	Cross-tier	Downlink
5	FUE	FBS	Co-tier	Uplink
6	FBS	FUE	Co-tier	Downlink

2.4 Interference Management Methods

In order to meet the high capacity of the network, the femtocells must incorporate the following interference management techniques:

(1) To avoid co-tier interference, each FAP impose a limitation on the transmitting power of FUE after gathering information from the surrounding FAPs. In case of cognitive OFDMA femtocells, FAP sense the environment for certain sub channels, if they are available, allocate to user which reduce the interference upto a significant level.

(2) To mitigate cross-tier interference, spectrum splitting technique is purposed, but it is not a sufficient technique because the spectrum is precious and very costly. In spectrum splitting, both femtocells and macrocells use different portion of spectrum that reduces the cross-tier interference.

Hence there is a need of some efficient interference avoidance scheme,

which reduce the co-tier and cross-tier interference to a significant level using co-channel deployment of femtocells and without compromising the spectral efficiency of the system.

Chapter 3

Background and Literature Review

3.1 Introduction

A complete introduction about femtocells including all types of interference scenarios is presented in [25], along with other papers such as [26][27][3][14]. Regarding interference avoidance in femtocells, many researchers proposed different frequency planning techniques. Initially, it was proposed to assign different orthogonal frequencies to the base stations of different cells [28]. We will discuss different frequency allocation schemes proposed by the researchers to avoid the interference in detail.

3.2 Fractional Frequency Reuse (FFR)

Authors in [29] proposed another elegant scheme of fractional frequency reuse (FFR). In FFR, whole of the spectrum is divided into multiple frequency

bands. These bands are distributed among cluster such that the users that are present in the middle of the cell are allocated with a separate band from the users that are present at the edge. Although this schemes allocates different frequency bands to the edgeusers and the users present in the center of the cell, but still it is spectrally inefficient as the available resources may not be used efficiently. it is shown in Figure 3.1.

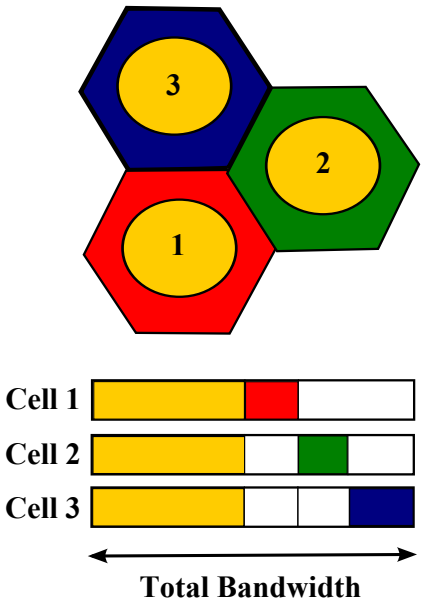

Figure 3.1: Fractional frequency reuse (FFR) [29]

3.3 Soft Fractional Frequency Reuse (SFFR)

The authors of [30] proposed soft fractional frequency reuse scheme. This schemes also partitions the whole frequency spectrum but allows the center-cell users to use more than one frequency bands. It is spectrally more efficient as compared to previous scheme because femto users can also utilize the same

band that is assigned to the macro users. The whole band is utilized within a single cell, which also makes it spectrally more efficient. The drawback of this scheme is that part of band is still statically dedicated for femto users and also like the previous schemes, this scheme does not take account of user's traffic distribution.

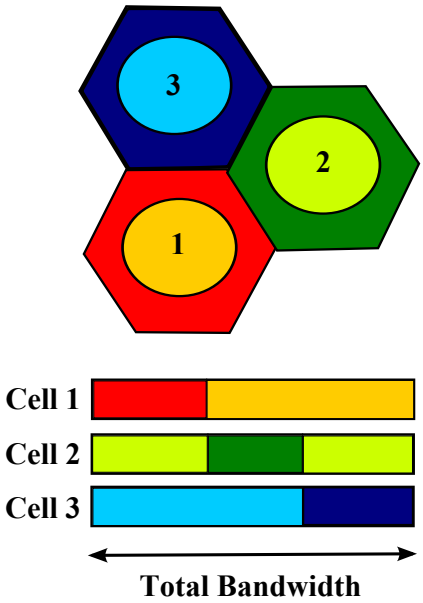

Figure 3.2: Soft fractional frequency reuse (SFFR) [30]

3.4 Power Control Algorithm

The authors of [31] proposed a simple algorithm which provides more preference to the MUEs by controlling the power of the FAP. The fundamental assumption is that, MBS provides the information of MUEs to all the FAPs. Once the MUEs is under significant interference, the nearby FAP will reduce its transmit power. This approach leads to the performance degradation of

FUEs. It is shown in Figure 3.3.

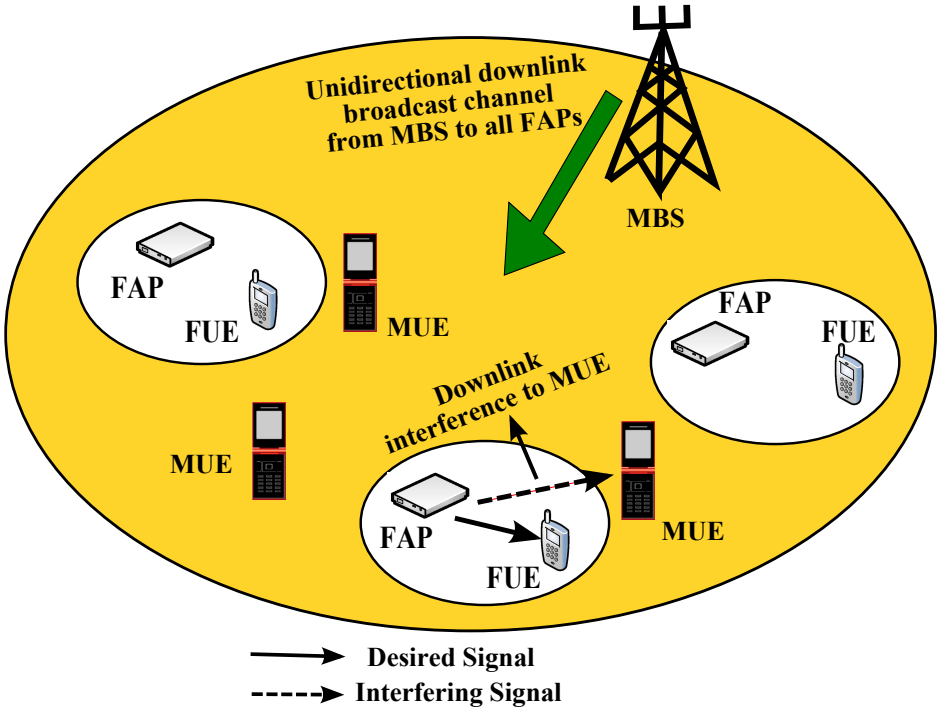

Figure 3.3: Downlink power control scheme [31]

3.5 Subchannel Allocation

Another approach which is used to avoid the interference in OFDMA based femtocells is discussed in [14]. In this approach, each FAP initially sense the surrounding radio environment for specific sub-channel. Each user equipment requires a certain number of sub-channels depending upon the QoS criteria. If a particular sub-channel is free, FAP then allocate the subchannel to that user, subject to low level of interference. This technique requires the cognitive capabilities that does not yield a cost effective solution.

3.6 Dynamic Frequency Reuse

The authors of [32] proposed a dynamic frequency reuse scheme that considers the overall traffic load. The spectrum allocation for both the macro and femto regions changes dynamically depending upon the traffic load pattern. However, the drawback of this scheme is that it is highly dependent upon current information about geographical locations of the users.

3.7 Static Frequency Band Allocation

In this scheme both femtocells and the macrocells operate in their dedicated spectrum [33]. In this case there will be no cross tier interference but the fundamental draw back is that the available spectrum is not efficiently used to meet the increasing data demand of the network. The frequency allocation is shown in Figure 3.4.

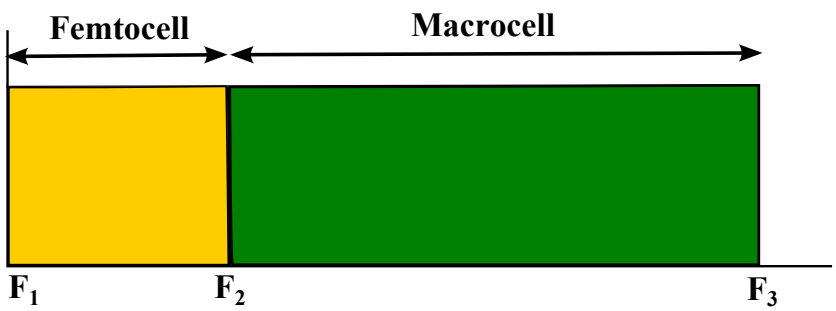

Figure 3.4: Frequency allocation using dedicated frequency band scheme [33]

3.8 Shared Frequency Band Allocation

This scheme allows the sharing of available spectrum among the femtocells and macrocells. It provides the efficient utiliztion of resources but in this case the co-tier and cross-tier interference will be high [33]. The frequency allocation is shown in Figure 3.5.

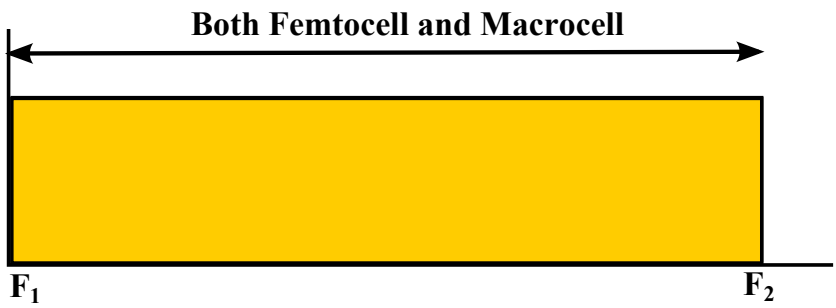

Figure 3.5: Frequency allocation using shared frequency band scheme [33]

3.9 Subset Frequency Band Allocation

In subset frequency band scheme, the whole spectrum is allotted to macrocell while a portion of the whole band is fixed for the femtocells. Although it is efficient reuse of available spectrum but again in this case the interference will be high [33]. The frequency allocation is shown in Figure 3.6.

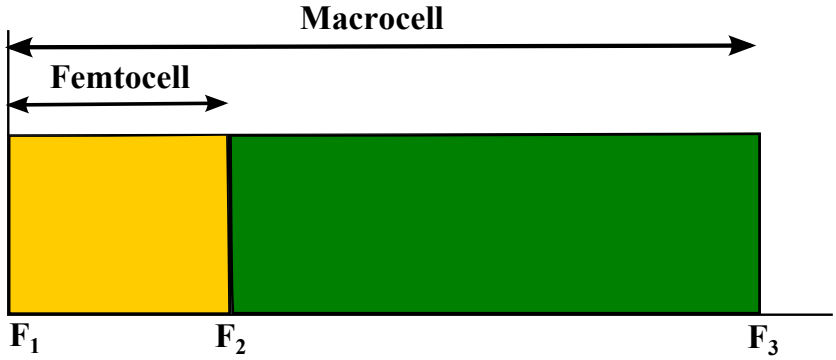

Figure 3.6: Frequency allocation using subset frequency band scheme [33]

3.10 Reverse Frequency Allocation Scheme

Technique that is analyzed in [34] is reverse frequency allocation scheme (RFA). Reverse Frequency allocation scheme divides the complete region into two non-over-lapping regions named as inner region and outer region. It is spectrally most efficient among all the schemes because it not only utilizes whole frequency band among single cell but also the frequencies used for the uplink and the downlink transmissions of MBS to MUE are being utilized as the downlink and uplink frequencies of FAP to FUE, respectively. The major draw back in this study is that the authors did not provide the analysis for higher multiple regions. Moreover, authors did not provide some closed-form mathematical expressions to capture the important metrices like SINR, coverage probability and average rates etc.

All the study that are mentioned above are mostly the simulation based. Authors have been used the monte carlo method to provide the simulation results. They did not provide the closed-form mathematical expressions to capture the coverage probability, SINR statistics and throughput of the net-

work.

In [35] authors proposed a general K-tier downlink model for HetNets that gives the simple mathematical expessions for most of the important metrices like SINR statistics, coverage probability and average rates. But the model do not consider frequency reuse, power control or any other form of the interference management techniques.

A well accepted and most popular model is the conventional two dimensional hexagonal grid model. This model is extensively used for system level simulations [36]. Another model that allows the random deployment of base stations in form of Poisson point process (PPP) [37]-[39]. Such models are more accurate and suitable for random deployment of femtocells. Moreover, the difference between random and actual deployment of base stations is small, even for macro base stations (MBSs) deployment. Recent research [40] showed that the deployment of macrocell base stations (MBSs) drawn from PPP is accurate as two dimensional hexagonal grid model, when compared to actual 4G network. The model also enables us to use the important mathematical tools from stochastic geometry to perform the analysis of HetNets more accurately [41][42]. This model has also been extended to obtain the results of coverage probability for femto-cellular networks, when a typical FUE connects to its nearest FAP [43].

In this thesis we study the downlink performance of a heterogeneous network by proposing a Reverse frequency allocation (RFA) scheme by dividing the cell service area into multiple regions and assign frequencies to various cell entities in such a way that the major interference is avoided. We analyze and evaluate the achievable performance of this technique for the

downlink scenario. Using simulations, we show that under reasonable signal-to-interference plus noise ratio (SINR) values, multiple regions enhance the performance of users by decreasing the overall system outage probability. It is shown that a 4-region RFA scheme provides almost double performance gain over a 2-region RFA scheme for the same set of parameters. Moreover, we provide a multiple region 2-tier downlink model using RFA scheme. We derive a closed-form expression for the coverage probability of femtocell user equipment (FUE) using different RFA schemes under open access mode. Where FAPs and MUEs are modeled as independent Poisson point process (PPP). Using simulations, we show that for reasonable values of signal-to-interference ratio, multiple regions enhance the coverage probability of an FUE. It is shown that a 4-region RFA outperforms the other RFA schemes at different densities of FAPs and MUEs as well as for different values of threshold for the same set of parameters.

Chapter 4

System Architecture

4.1 Introduction

In this chapter we provide the complete performance analysis of RFA scheme with multiple regions and compare it with 2-region RFA scheme. We consider a reverse frequency allocation (RFA) scheme for a single cell in which the entire region of a macrocell is divided into k disjoint regions. Furthermore, the allocated frequency spectrum, F, is divided among k orthogonal sub-bands, such that $F = \bigcup_{i=1}^{k} F_i$, where $\bigcap_{i=1}^{k} F_i = \phi_i$; ϕ denotes a empty set.

For every ith region, we assume frequency division duplexing (FDD), i.e., each sub-band is further divided into its uplink and downlink frequency bands, such that $F = [F_{iA} + F_{iB}]$; where $i = \{1, 2, ...K\}$ For a fair usage of frequencies in the RFA scheme, we assume $k = 2^M$, where $M \in Z^+ = \{1, 2, ...\}$.

In the following, we consider k=4 and provide a complete spectral decomposition of the network for a 4-region RFA scheme. As mentioned earlier, the

F1		F2		F3		F4	
R1 Macrocell UL	R1 Macrocell DL	R2 Macrocell UL	R2 Macrocell DL	R3 Macrocell UL	R3 Macrocell DL	R4 Macrocell UL	R4 Macrocell DL
F_{1A}	F_{1B}	F_{2A}	F_{2B}	F_{3A}	F_{3B}	F_{4A}	F_{4B}
R3 Femtocell DL	R3 Femtocell UL	R4 Femtocell DL	R4 Femtocell UL	R1 Femtocell DL	R1 Femtocell UL	R2 Femtocell DL	R2 Femtocell UL

Figure 4.1: Reverse frequency allocation of 4 regions.

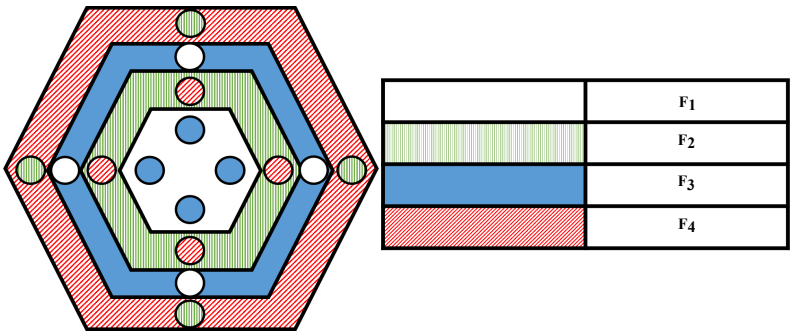

Figure 4.2: Frequency distribution for 4 regions.

basic aim of the RFA scheme is to divide a cellular region in such a way that least amount of interference scenarios are produced; thereby decreasing the overall outage of the system. For that as shown in Figure 4.1, the available region is divided into four non overlapping regions, i.e., R_1, R_2, R_3, and R_4, respectively. The available spectrum F for the single cell is also divided into 4 bands namely F_1, F_2, F_3, and F_4 and each region is assigned a frequency band. Each band contains the uplink and downlink frequency carriers. Frequency carriers F_{1A} and F_{1B} are used by MUEs in R_1, F_{2A} & F_{2B} for MUEs in R_2 for uplink and downlink operations, and so on. It can be observed that the MBS have relatively high transmit power as compared to FAPs, hence the femto users recieve large amount of interference from MBS on the same

frequency channel. Thus it is desired to allocate the frequencies in such a way that a femto user receives no interference from the downlink of MBS. Hence if F_{1A} is used for downlink FUEs in R_3, it is desired to reuse this frequency for one of the uplinks of MUEs in R_1, and interference is minimal if these two interfering regions are as far as possible. Hence we make two sets of interfering regions; R_1 & R_3, and R_2 & R_4. Hence this implies that R_1-FUE in downlink uses the same frequency as the uplink MUE in R_3.

Since our focus for this study is the downlink receiver (mobile users either MUEs or FUEs), hence the interference arrives from R_3-FAP to R_1-MUE. As FAPs are low powered and large path loss exists between these nodes this interference is not significant. On the other hand, the R_1-MUE in uplink uses the same frequency as that of the downlink FUE in R_3. In this case, the downlink FUE recieves interference from MUE uplink, which is again low-powered and feeble because of the path loss between R_1 and R_3. Hence minimal interference is observed using this scheme for both downlink users, i.e, R_1-MUE and R_3-FUE. Same procedure is done for R_2 and R_4. In summary, the frequencies are allocated to the femtocells in such a way that the femtocells that are contained in R_1 will use F_{3A} and F_{3B} frequency carriers for their downlink and uplink operations, respectively. Similarly, R_2 femtocells will use F_{4A} and F_{4B} frequency carriers for downlink and uplink operations, respectively. In the same way, R_3 and R_4 femtocells will utilize F_{1A}, F_{1B} and F_{2A}, F_{2B} frequency carriers for their downlink and uplink operations, respectively.

4.2 Interference Modeling and Region Selection

As described earlier, the intereference in this particular case of 4-region RFA arrives from only one interfering region. For example, communication going on in R_1 will be interfering the communication of R_3 as they are operating on the same partitioned frequency, i.e., F_1. Interference, on the other hand, will be significantly reduced because in the 4-region case the area under each region is minimized. As the area is reduced the number of interferers will also be reduced on the average.

Although the RFA scheme offers more vulnerability to interference, however, interference either co-tier and/or cross-tier both will have their impact on the downlink users performance metrics. These performance metrics can be throughput and coverage etc. In heterogeneous networks a designer must, due to different channel conditions, prioritize these performance metrics. For example, in an enviroment of high user density the system must optimize its spectral effeciency so that greater number of users can be adjusted. While on the other hand a system that ensures high data rate must optimize to certify high SINR. In each case the other performance metric can be sub-optimized.

We now model the various types of interferences present in our system. As described, the FUEs encounter interference not only from uplink MUEs in the distant region but also from the neighboring FAPs in the same region that are operating at the same frequency. As this paper studies the outage aspects of the network, which means that the SINR is the performance metric that will be used in this type of system. The SINR at a reciever j can be

calculated as

$$SINR(dB) = \frac{P_{des}}{d_{des}^{\beta}}\mu_{mj} - \sum_{i\in \mathbb{I}} \frac{P_i}{d_{ij}^{\beta}}\mu_{ij} \tag{4.1}$$

where P_{des} is the power recieved from the intended transmitter m, while P_i is the interfering power from the ith transmitter, which can be co-tier or cross-tier interferer. The set $\mathbb{I}$ denotes the set of all interferers. The path loss exponent is represented as β, while the distances of the reciever from the interferers and desired transmitter are represented as d_{ij} and d_{des}, respectively. The flat fading channel gain from the desired and interfering transmitter to the jth receiver is denoted by μ_{mj} and μ_{ij}, respectively, where μ_{mj} , $\mu_{ij} \in \mu$ and the set μ consists of independently and identically distributed (i.i.d) random variables, which are drawn from an exponential distribution with the parameter σ_{μ}^2 =1. Hence we are intrested in finding the $\mathbb{P}\{SINR \leq P_{th}\}$ and average this outage probability for all users of the system.

4.2.1 Optimal Partitioning of Regions

The multiple regions in the RFA must be partitioned in such a way that the impact of the interference should be minimized. For example, in Figure 4.3, 4-region RFA is implemented in a cell with radius r, which is further divided into four non-overlapping regions. To find the optimal distance for each region, we consider a worst-case scenario, i.e., we want to calculate the optimal region lengths, when the interference in the system is maximum. As it is already been shown that the in a 4-region RFA, R_1 and R_2 are the interfering regions with R_3 and R_4, respectively. The femto users (FUEs) are placed at the region boundries while their interfering macro users (MUEs) are placed

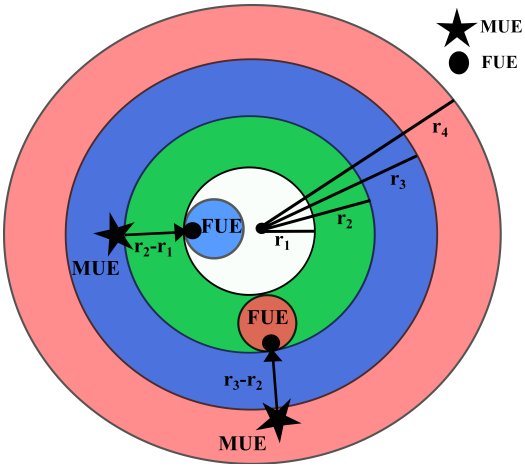

Figure 4.3: Worst-case scenario in 4-region RFA. The direction of arrows shows the interference direction.

at their nearest interfering region's boundry. This is the worst-case scenario because the interference from each MUE to its respective FUE is maximum in this situation. As the co-tier interference is one of the major contributing factors towards the total interference in this RFA scheme and will have a significant impact in R_1. This is due to the fact that the density of the femtocells with respect to this area is highest in this region. So for a certain fixed threshold, P_{th}, through extensive simulations, it is observed that r_1 should be atleast $0.6r$ so that the SINR of this particular region sould be above an acceptable value. As in the worst-case, SINR should be at least equal to the P_{th} to get success, therefore, our optimization problem becomes the following;

$$maximize \ \{SINR\}$$

$$s.t$$

$r_1 = 0.6r, \ r_1 \leq r_2 \leq r_3 \leq r_4$ and $r_4 = r$, where r_1, r_2, r_3 and r_4 are the radius of R_1,R_2, R_3 and R_4 regions, respectively. To explain this approach, let us

again consider the example of 4-region RFA. From Figure 4.3,

$$SINR_{opt} = \frac{(r_2 - r_1)^2}{\delta_{FUE}} = P_{th}, \tag{4.2}$$

$$SINR_{opt} = \frac{(r_3 - r_2)^2}{\delta_{FUE}} = P_{th}, \tag{4.3}$$

where δ_{FUE} is the maximum distance of FUE from its intended FAP. From (4.2) and (4.3),

$$r_2 = \frac{(r_1 + r_3)}{2}. \tag{4.4}$$

As, $r_3 \leq r_4$ then $r_2 \leq 0.8r$. Now r_3, due to fairness, is taken equal between r_2 and r_4. So, $r_3 \leq\ 0.9r$.

Chapter 5

Stochastic Modeling of Multiple Region RFA

5.1 Introduction

As mentioned earlier, the RFA scheme divides the entire cell into K non-overlapping regions. Likewise, the available frequency spectrum, F, is divided into K frequency subbands, such that $F = \bigcup_{i=1}^{K} F_i$. The K frequency subbands are further divided into uplink and downlink frequency carriers for every ith region, such that $F = [F_{iA} + F_{iB}]$; where $i = \{1, 2, ...K\}$.

In case of 2-RFA, the two disjoint regions R_1 and R_2 are assigned subbands F_1 and F_2, respectively. The uplink band of R_1-MUEs is reused by the downlink FUEs in R_2. Similarly, the uplink band of R_2-MUEs is reused by the downlink FUEs in R_1. Using such frequency allocation, the FUEs receive interference from a subset of uplink MUEs that are using the same frequency carriers, instead of MBS, which is a great source of interference. Similar procedure is followed in the other subbands, i.e., the downlink MUEs

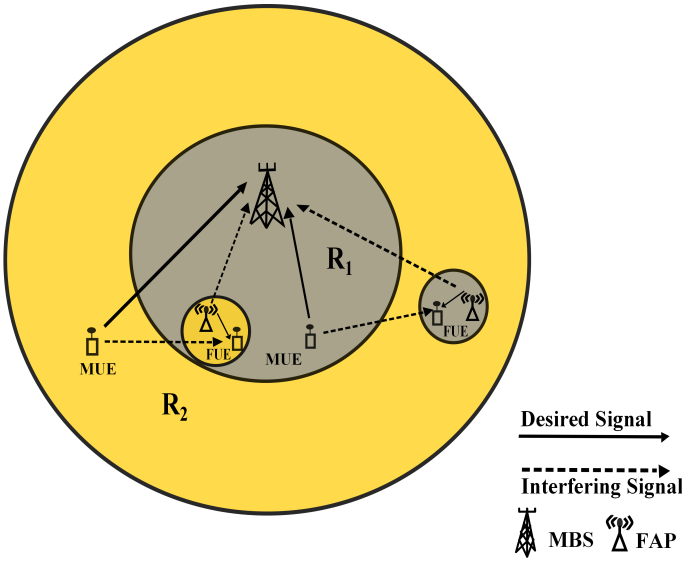

Figure 5.1: 2-RFA interfering scenarios; only downlink FUEs scenarios are shown.

in R_1 utilize the same band as FUEs for uplink in R_2 and the downlink MUEs in R_2 use the same band as uplink FUEs in R_1. In this case the downlink MUEs in R_1 and R_2 only face the cross-tier interference from a subset of uplink FUEs in R_2 and R_1, respectively.

We consider a worst case scenario for FUEs in both regions, in which all the uplink MUEs in R_2 and neighboring downlink FAPs in R_1 produce the cross-tier and co-tier interference to the R_1-FUEs, repectively. The same is the case with R_2-FUEs, i.e., all the uplink R_1-MUEs and neighboring downlink FAPs in R_2 generate the cross-tier and co-tier interference, respectively. Since all the FAPs in R_1 and R_2 are operating on the same frequency carriers F_{2A} and F_{1A} for downlink, respectively, so co-tier interference will also occur. Hence the FUEs in each region receive two types of interferences, one is the co-tier interference from neighboring FAPs in the same region, and other is

the cross-tier interference from MUEs in the other region.

Similarly, in the case of 4-RFA, an entire cell is divided into four disjoint regions. i.e., R_1, R_2, R_3 and R_4 and likewise the spectrum. The four sub-bands are further divided into uplink and downlink frequency carriers. i.e., $F = [F_{iA} + F_{iB}]$; where $i = \{1, 2, ...4\}$. Now F_{1A} and F_{1B} are used by MUEs for uplink and downlink in R_1, F_{2A} and F_{2B} are used by the MUEs in R_2 for uplink and downlink, respectively. The same is the case for MUEs in R_3 and R_4. Since F_{1A} and F_{1B} are used by the R_1-MUEs for uplink and downlink operations, so it is desired to reuse these frequency carriers to one of the downlinks and uplinks of FUEs in a distant region R_3, respectively. Similarly, F_{2A} and F_{2B} which are used by the MUEs in R_2 for uplink and downlink are also utilized by the R_4-FUEs for downlink and uplink operations, respectively. In case of R_1-MUEs, they receive interference from uplink FUEs in R_3 while R_2-MUEs receive interference from uplink FUEs in R_4. Hence we make two interfering regions; R_1 & R_3 and R_2 & R_4. The interference will be minimum if the interfering regions are as far as possible.

In summary, R_1-FUEs and R_2-FUEs receive interference from the uplink MUEs in R_3 and R_4, respectively. The R_3-FUEs and R_4-FUEs receives interference from the uplink MUEs in R_1 and R_2, respectively. The R_1-MUEs and R_2-MUEs receive interference from the uplink FUEs in R_3 and R_4, respectively, while R_3 and R_4-MUEs receive interference from uplink FUEs in R_1 and R_2, respectively.

Table 5.1: 4-RFA interference scenarios

Scenarios	**FUE location**	**Interference**
First	FUE in R_1	uplink MUEs in R_3 & downlink FAPs in R_1
Second	FUE in R_2	uplink MUEs in R_4 & downlink FAPs in R_2
Third	FUE in R_3	uplink MUEs in R_1 & downlink FAPs in R_3
Fourth	FUE in R_4	uplink MUEs in R_2 & downlink FAPs in R_4

5.2 Stochastic Modelling of the Network

Consider a 4-RFA downlink geometry of a 2-tier HetNet for a single cell. The first tier is the macrocellular network while the femtocells form the second tier of the network. Each tier may differ on the values of transmit power, thresholds and user densities per unit area.

In this study, we are intrested in calculating the average success probability of an FUE when the FUE is placed in any region of the 4-RFA network and receives co-tier and cross-tier interferences as discussed in the previous section. Since there are four regions in 4-RFA, four FUE location scenarios arise, which are shown in Table 5.1. In the following, we discuss the first scenario by assuming the worst case in which R_1-FUE receives interference from all the neighboring downlink FAPs in the same region R_1 and from all the uplink MUEs in R_3. Without the loss of generality, we locate the FUE at origin, which connects to one FAP in R_1 only if its downlink received signal-to-interference plus noise ratio from that FAP is greater than a pre-defined threshold τ. Since the FUE, when connected to a FAP, gets interference from neighboring FAPs in R_1 and MUEs in R_3; we model the distribution of FAPs and MUEs as spatial PPPs, $\phi_j^{(i)}$, each having a density of $\lambda_j^{(i)}$, where j

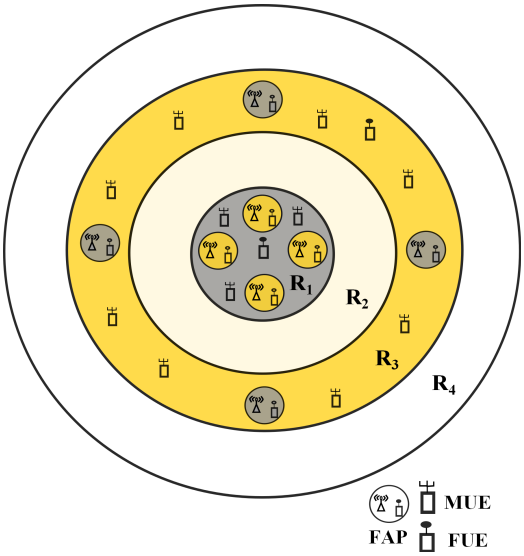

Figure 5.2: 4-RFA geometry of 2-tier Hetnet; only first scenario is shown.

denotes the tier of the network, $j \in \{1, 2\}$, and i denotes the ith region of a cell, where $i = 2^M$ and $M = \mathbb{Z}^+$. Hence for 4-RFA, $M = 2$ and $i = 4$. Thus for each of the four regions R_1, R_2, R_3 and R_4, we have two independent PPPs; one for uplink MUEs with density $\lambda_1^{(i)}$, and one for FAPs with density $\lambda_2^{(i)}$. We first divide the entire cell into four regions and then distribute the FAPs and MUEs as independent PPPs in each region. All the FAPs and MUEs have equal density in each region. For example, for 1000 FAPs and MUEs, each region consists of 250 FAPs and MUEs, respectively. Moreover, we let r_1 be the radius of region R_1. Similarly r_i denotes the annulus region between $R_i - R_{i-1}$, $i \in \{2, 3, 4\}$.

Let $y_j^{(i)}$ denotes the set of all locations of FAPs or MUEs in the ith region. The downlink transmission of FAP undergoes Rayleigh fading and path loss. The squared envelope of the channel fading between two terminals is represented by $h_{y_j}^{(i)}$, which consists of independently and identically distributed

(i.i.d) random variables (RVs) that are drawn from an exponentional distribution. The path loss function is given by $\ell(y_j^{(i)}) = \| y_j^{(i)} \|^{-\alpha}$, where α is the path loss exponent. Therefore, the received signal-to-interference ratio for R_1-FUE is given as

$$\gamma = \frac{P_2 h_{y_2}^{(1)} \| y_2^{(1)} \|^{-\alpha}}{\sum_{y \in \phi_2^{(1)} \setminus y_2^{(1)}} P_2 h_y^{(1)} \| y \|^{-\alpha} + \sum_{y \in \phi_1^{(3)}} P_1 h_y^{(3)} \| y \|^{-\alpha}}. \tag{5.1}$$

where P_j is the transmit power of MUEs or FAPs for $j = 1$ and $j = 2$, respectively. The reason for considering SIR is that the self interference dominates the noise in cellular networks even with modest density, hence we ignore the effects of thermal noise in the sequel. We now present the coverage probability of an FUE as the following theorem.

Theorem

Theorem 5.1. *The coverage probability of R_1-FUE in a 4-RFA scenario under SIR connectivity is given by*

$$P_c \leq \frac{\lambda_2^{(1)} \pi}{A} \left[1 - \exp(-A r_1^2) \right]$$

where

$$A = \left(\frac{\tau}{P_2} \right)^{2/\alpha} \left(C_1^{(3)} \lambda_1^{(3)} (P_1)^{2/\alpha} + C_2^{(1)} \lambda_2^{(1)} (P_2)^{2/\alpha} \right)$$

$$C_1^{(3)} = 2\pi \int_{r_2}^{r_3} \frac{r}{1 + r^\alpha} \mathrm{d}r, \text{ and } C_2^{(1)} = 2\pi \int_0^{r_1} \frac{r}{1 + r^\alpha} \mathrm{d}r.$$

Proof. The coverage probability is given as

$$
\begin{aligned}
P_c &= \mathbb{P}\left(\bigcup_{y_2^{(1)} \in \phi_2^{(1)}} \gamma(y_2^{(1)}) > \tau \right) \\
&= \mathbb{E}\left[\mathbf{1}\left(\bigcup_{y_2^{(1)} \in \phi_2^{(1)}} \gamma(y_2^{(1)}) > \tau \right) \right. \\
&\leq \mathbb{E} \sum_{y_2^{(1)} \in \phi_2^{(1)}} \left(\gamma(y_2^{(1)}) > \tau \right) \\
&= \lambda_2^{(1)} \int_{R^2} \mathbb{P}\left(\frac{P_2 h_{y_2}^{(1)} \ell(y_2^{(1)})}{I_y} > \tau \right) \mathrm{d}y_2^{(1)} \qquad (5.2) \\
&= \lambda_2^{(1)} \int_{R^2} \mathcal{L}_{I_y}\left(\frac{\tau}{P_2 \ell(y_2^{(1)})} \right) \mathrm{d}y_2^{(1)}, \qquad (5.3)
\end{aligned}
$$

where inequality is due to the fact that for SIR threshold $\tau \geq 1$, the equality holds, otherwise the right hand side becomes the upper bound of the coverage probability and (5.2) follows from the Campbell Mecke Theorem [41] and (5.3) follows from the assumption that the channel gains are assumed to be Rayleigh distributed. Here I_y is the cumulative interference that includes both co-tier and cross-tier inteference and $\mathcal{L}_{I_y}(.)$ is the Laplace transform of the cumulative interference from all the interferers of both tiers, when an FUE is connected to its desired FAP. Since the PPPs are stationary, hence the interference is not dependent upon the location y. Therefore, $\mathcal{L}_{I_y}(.)$ is represented by $\mathcal{L}_I(.)$, which is further given as

$$
\begin{aligned}
\mathcal{L}_I(s) = \mathbb{E}&\left[\prod_{y \in \phi_1^{(3)}} \exp(-sP_1 h_y^{(3)} \ell(y)) \right] \\
\times \mathbb{E}&\left[\prod_{y \in \phi_2^{(1)} \setminus y_2^{(1)}} \exp(-sP_2 h_y^{(1)} \ell(y)) \right], \qquad (5.4)
\end{aligned}
$$

As the fading random variables are independent, so (5.4) becomes

$$\mathcal{L}_I(s) = \mathbb{E}_{\phi_1^{(3)}}\left[\prod_{y\in\phi_1^{(3)}} \mathbb{E}_h[\exp(-sP_1 h_y^{(3)}\ell(y))]\right] \times\mathbb{E}_{\phi_2^{(1)}}\left[\prod_{y\in\phi_2^{(1)}\setminus y_2^{(1)}} \mathbb{E}_h[\exp(-sP_2 h_y^{(1)}\ell(y))]\right], \tag{5.5}$$

$$\mathcal{L}_I(s) = \mathbb{E}_{\phi_1^{(3)}}\left[\prod_{y\in\phi_1^{(3)}} \frac{1}{1+sP_1\ell(y)}\right] \times\mathbb{E}_{\phi_2^{(1)}}\left[\prod_{y\in\phi_2^{(1)}\setminus y_2^{(1)}} \frac{1}{1+sP_2\ell(y)}\right], \tag{5.6}$$

where (5.6) follows from the assumption that the channel gains are Rayleigh faded. We now have

$$\mathcal{L}_I(s) = \exp\left(-\lambda_1^{(3)}\int_{r_2}^{r_3}\left(1-\frac{1}{1+sP_1 \parallel y_1^{(3)} \parallel^{-\alpha}}\right)\mathrm{d}y_1^{(3)}\right) \times \exp\left(-\lambda_2^{(1)}\int_{0}^{r_1}\left(1-\frac{1}{1+sP_2 \parallel y_2^{(1)} \parallel^{-\alpha}}\right)\mathrm{d}y_2^{(1)}\right), \tag{5.7}$$

where (5.7) follows from the probability generating functional (PGFL) of underlying PPPs [41]. Eq. (5.7) can be rewritten as

$$\mathcal{L}_I(s) = \exp\left(-2\pi\lambda_1^{(3)}(sP_1)^{2/\alpha}\int_{r_2}^{r_3}\frac{r}{1+r^\alpha}\mathrm{d}r\right) \times \exp\left(-2\pi\lambda_2^{(1)}(sP_2)^{2/\alpha}\int_{0}^{r_1}\frac{r}{1+r^\alpha}\mathrm{d}r\right), \tag{5.8}$$

where (5.8) results from converting the cartesian coordinates to polar coordinates. It can be further simplified as

$$\mathcal{L}_I(s) = \exp\left[-(s)^{2/\alpha}C_1^{(3)}\lambda_1^{(3)}(P_1)^{2/\alpha}\right] \times \exp\left[-(s)^{2/\alpha}C_2^{(1)}\lambda_2^{(1)}(P_2)^{2/\alpha}\right], \tag{5.9}$$

where

$$C_1^{(3)} = 2\pi \int_{r_2}^{r_3} \frac{r}{1+r^\alpha} \mathrm{d}r,$$

and

$$C_2^{(1)} = 2\pi \int_{0}^{r_1} \frac{r}{1+r^\alpha} \mathrm{d}r.$$

For a special case of $\alpha = 2$,

$$C_1^{(3)} = \pi \log\left[\frac{1+r_3^2}{1+r_2^2}\right], \; and \; C_2^{(1)} = \pi \log\left[1+r_1^2\right].$$

For other values of α, $C_j^{(i)}$'s can be computed numerically. By using (5.3) and (5.9), the coverage probability of R_1-FUE is given by

$$P_c^{(1)} \leq \lambda_2^{(1)} \int_0^{r_1} e^{\left(-\left(\frac{\tau}{P_2}\right)^{2/\alpha}\left(C_1^{(3)}\lambda_1^{(3)}(P_1)^{2/\alpha}+C_2^{(1)}\lambda_2^{(1)}(P_2)^{2/\alpha}\right)\|y_2^{(1)}\|^2\right)} \mathrm{d}y_2^{(1)}. \quad (5.10)$$

By solving the integeral, (5.10) can be further simplified to

$$P_c \leq \frac{\lambda_2^{(1)}\pi}{A}\left[1-\exp(-Ar_1^2)\right]. \quad (5.11)$$

■

In the second scenario, R_2-FUE receives the interference from all the neighboring downlink FAPs in the same region R_2 and from all the uplink MUEs in R_4. Hence using the same procedure as previously described, the coverage probability of the R_2-FUE is given by

$$P_c^{(2)} \leq \lambda_2^{(2)} \int_{r_1}^{r_2} e^{\left(-\left(\frac{\tau}{P_2}\right)^{2/\alpha}\left(C_1^{(4)}\lambda_1^{(4)}(P_1)^{2/\alpha}+C_2^{(2)}\lambda_2^{(2)}(P_2)^{2/\alpha}\right)\|y_2^{(2)}\|^2\right)} \mathrm{d}y_2^{(2)}. \quad (5.12)$$

where

$$C_1^{(4)} = 2\pi \int_{r_3}^{r_4} \frac{r}{1+r^\alpha} \mathrm{d}r, \; and \; C_2^{(2)} = 2\pi \int_{r_1}^{r_2} \frac{r}{1+r^\alpha} \mathrm{d}r.$$

Similarly, in case of third and fourth scenario the coverage probability of FUE is given by

$$P_c^{(3)} \leq \lambda_2^{(3)} \int_{r_2}^{r_3} e^{\left(-\left(\frac{\tau}{P_2}\right)^{2/\alpha}\left(C_1^{(1)}\lambda_1^{(1)}(P_1)^{2/\alpha}+C_2^{(3)}\lambda_2^{(3)}(P_2)^{2/\alpha}\right)\|y_2^{(3)}\|^2\right)} \mathrm{d}y_2^{(3)}. \quad (5.13)$$

where

$$C_1^{(1)} = 2\pi \int_0^{r_1} \frac{r}{1+r^\alpha}\mathrm{d}r, \; and \; C_2^{(3)} = 2\pi \int_{r_2}^{r_3} \frac{r}{1+r^\alpha}\mathrm{d}r.$$

$$P_c^{(4)} \leq \lambda_2^{(4)} \int_{r_3}^{r_4} e^{\left(-\left(\frac{\tau}{P_2}\right)^{2/\alpha}\left(C_1^{(2)}\lambda_1^{(2)}(P_1)^{2/\alpha}+C_2^{(4)}\lambda_2^{(4)}(P_2)^{2/\alpha}\right)\|y_2^{(4)}\|^2\right)} \mathrm{d}y_2^{(4)}. \quad (5.14)$$

where

$$C_1^{(2)} = 2\pi \int_{r_1}^{r_2} \frac{r}{1+r^\alpha}\mathrm{d}r, \; and \; C_2^{(4)} = 2\pi \int_{r_3}^{r_4} \frac{r}{1+r^\alpha}\mathrm{d}r.$$

Chapter 6

Simulation Results and Performance Analysis

6.1 Introduction

In this chapter, we present the performance analysis and simulation results of 4-RFA and compare it with 2-RFA scheme. It is shown that the proposed 4-RFA scheme outperforms the 2-RFA scheme in dense femtocell deployment scenarios. In our simulation enviroment, we randomly distribute circular-shaped femtocells within a hexagonal macrocell. Open access mode is simulated in our simulations for the femtocells. Macrocell base station (MBS) and femto access points (FAPs) are assumed to have omnidirectional antennas. Transmission power of MBS and FAP is fixed to be 20 and 0.2 Watts, respectively, while the transmit power of both MUE and FUE is fixed to 0.2 Watts. The users are uniformly placed in the macrocell, where atleast one user is placed in each femtocell. Parameters used for the simulations are shown in Table 6.1. User outage for 2-region and 4-region RFA is analyzed.

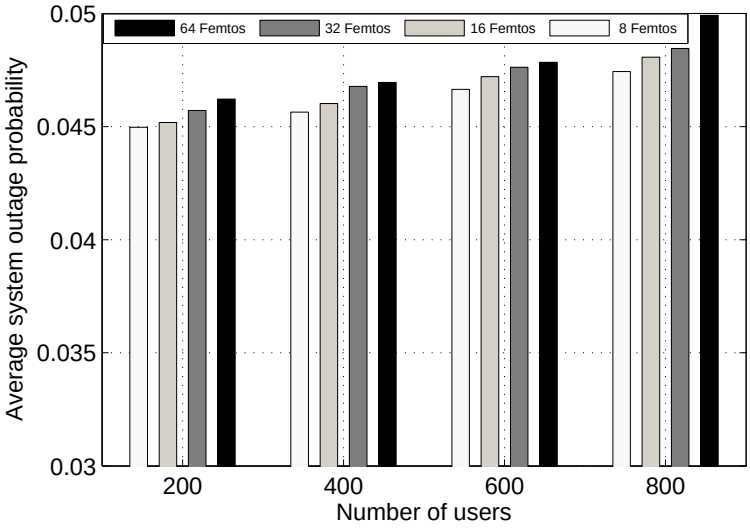

Figure 6.1: Average system outage probability of 2 region RFA.

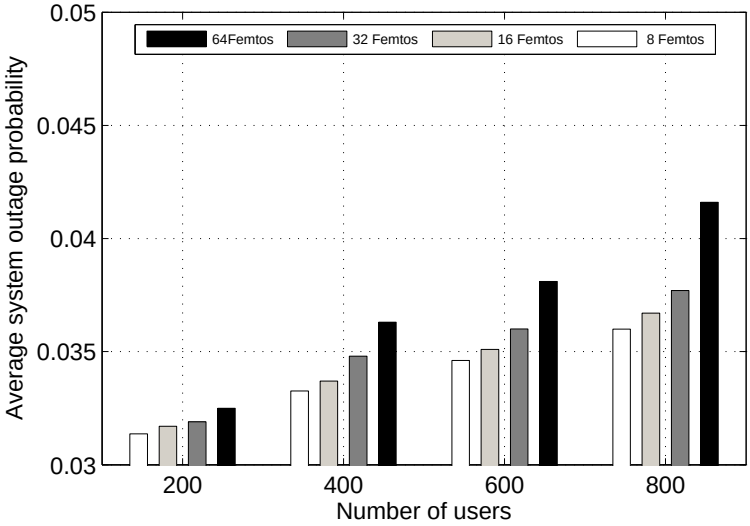

Figure 6.2: Average system outage probability of 4 region RFA.

Figure 6.1 and 6.2, shows the outage probability in a 2-region RFA scheme with the 4-region RFA. These graphs analyze the overall system outage for

Table 6.1: Simulation Parameters

Parameter	Value
Carrier Frequency	2500 MHz
Power of MBS	20 Watts
Power of MUE	0.2 Watts
Power of FAP	0.2 Watts
Power of FUE	0.2 Watts
Femto Radius	50 meters
Macrocell radius	1 to 4 km
Threshold value	-50dB

a macrocell having a radius of 1Km with varying number of users and with varying total number of femtocells. The path loss exponent, β, is taken to be 2 in this case. It can be observed that as the number of users increases, the average system outage probability also increases. This increase in the system outage is due to the cross-tier interference, i.e., interference from MUEs to FUE in the uplink direction. Also with the increasing number of femtocells, the co-tier interference also increases, i.e., interference from FAPs to FUEs in the downlink direction. Therefore, in both cases, i.e, either increasing number of users and/or femtocells, the system outage probability increases.

In Figure 6.1, 2-region RFA scheme is analyzed. It divides the complete cell in 2 regions. Simulations were performed on different number of femtocells. For example, when 8 femtos are considered then each region contains 4 femtocells. Similarly, for 64 femtos, every region has 32 femtocells each and so on. From Figures 6.1 and 6.2, we can see that 4-region RFA scheme outperforms 2-region RFA in terms of system outage probability. This reduction in system outage is due to the fact that 4-region RFA divides the complete single cell in such a way that each region has less number of interferers.

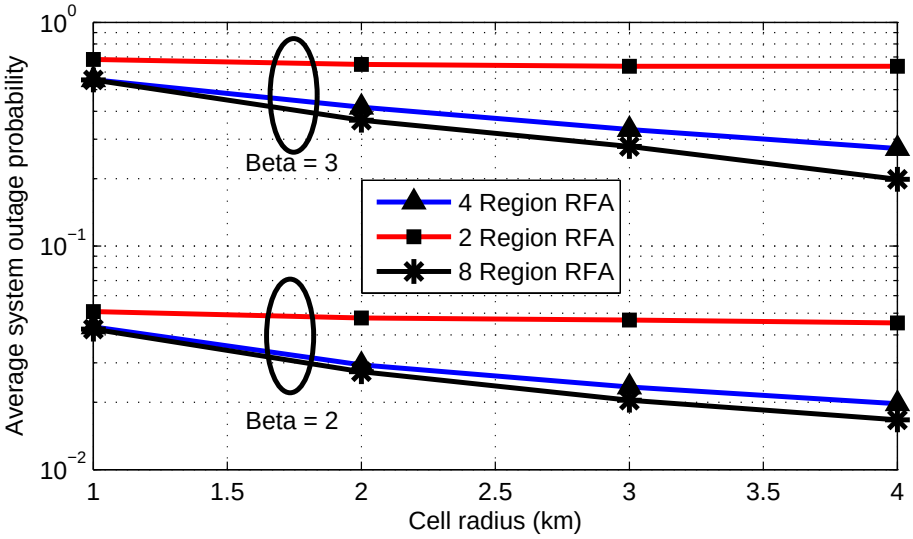

Figure 6.3: Average system outage probability at different cell radius.

Figure 6.3 analyzes different RFA schemes i.e., 2-region, 4-region, and 8-region RFA, at different cell radii and different path loss exponents. 800 users and 64 femtocells were randomly distributed in the cell. In 8-region RFA, total area is divided among 8 regions. Frequency spectrum is divided in such a way that any region, at maximum, can have no more than 2 interfering regions. For example, R_3 will have R_1 and R_5 as its interfering regions. Similarly, R_4 has R_2 and R_6 as its interfering regions. On the other hand R_1, R_2, R_7, and R_8 will have only one interfering region. As the cell radius increases, the distance between the FUE (victim) and the MUE and interfering FAPs (aggressor) also increases, alleviating the SINR of FUE. This improvement in performance is not as significant in 8-region RFA as it is in 4-region RFA scheme. This is due to the fact that as the number of regions increases for a fixed cell radius, not only the interfering regions come close but also the size of each region decreases, yielding higher co-tier and

cross-tier interferences. Hence at smaller cell radii 8-region RFA performs almost equal to the 4-region RFA scheme.

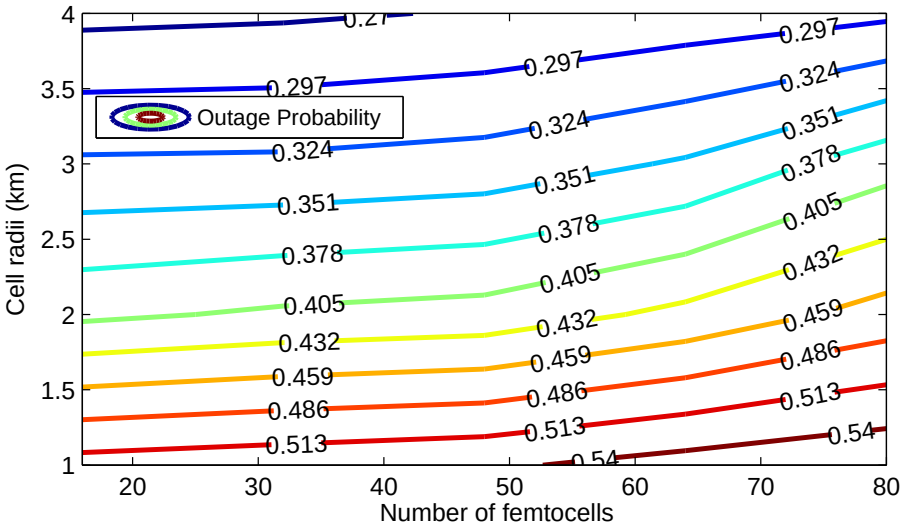

Figure 6.4: Average system outage probability at different users and cell radius.

On the other hand, it can also be seen that as the cell radius increases, the difference between the performance of 2-region and 4-region RFA also increases. For larger cell radii, the 4-region RFA significantly improves the performance in terms of outage probability. For example, at the cell radius of 4Km with 800 users and $\beta = 2$, the 2-region RFA scheme provides an average system outage probability approximately equal to 5%, but in the 4-region RFA with same parameters, the average system outage probability decreases to 2%. Hence large number of users will be in coverage. Similarly, for the larger path loss exponents, β, it can be seen that the 4-region RFA outperforms the 2-region RFA. For example, the difference in system outage probability for two schemes at a radius of 4Km with $\beta = 2$ is 3%. While

at $\beta = 3$, this difference is increased up to approximately 40%. So, we can say that for larger cell radius or larger path loss exponent, the 4-region RFA completely outperforms the 2-region RFA.

Figure 6.4 shows the contour plot that provides the average system outage probability that will be faced in any cell with a particular radius and varying number of femtocells for a 4-region RFA. These simulations were done with 600 users and β is taken to be 3. It can be observed that at a radius of $2Km$, the outage probability for 80 femtocells is around 46%. If this outage probability needs to be reduced for same number of cell users to 40%, then the maximum number of allowed femtocells should not be greater than 30. Hence an upper bound on the number of femtocells can be evaluated for varying cell radii.

6.2 Numerical results and performance analysis

In this section, we present our analytical results for 4-RFA and compare it with other reuse schemes. The transmission power of MUEs and FAPs is fixed to be unity. We conduct the analysis of coverage probability by locating the FUE in any region of the 4-RFA network. Moreover, we consider a worst-case scenario in which all the FAPs are operating at downlink while all the MUEs are operating at uplink in every ith region. The average coverage probability of FUE at different densities of FAPs and MUEs is analyzed for different RFA schemes. In 1-RFA scheme, there is a single cell area and the FUE connects to a FAP having SIR $> \tau$, whereas it receives interference

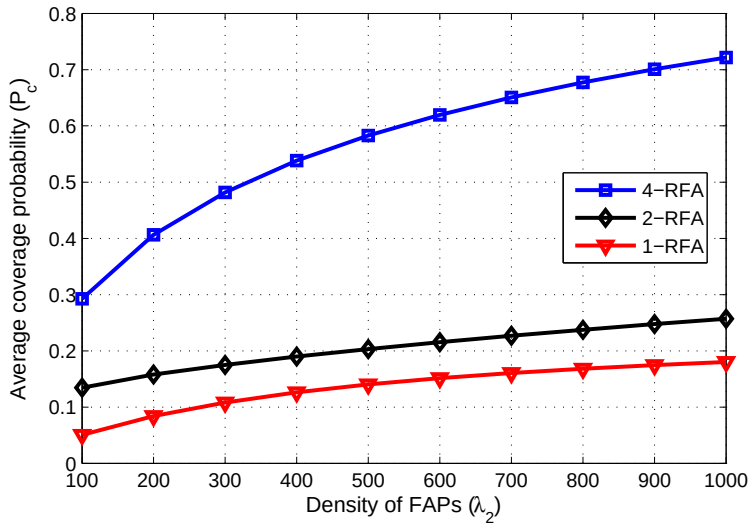

Figure 6.5: Average coverage probability of FUE at different density of FAPs (λ_2); ($\lambda_1 = 200$, $\tau = -6.98dB$)

from all other FAPs and MUEs in the same area.

Figures 6.5 and 6.6 shows the average coverage probability of an FUE by varying the densities of FAPs (λ_2) and MUEs (λ_1), in case of different RFA schemes. These graphs analyze the average coverage probability of FUE in a macrocell having a radius of $2Km$. The path loss exponent α is taken to be 2. The channel gains $h_{y_j}^{(i)}$are assumed to be Rayleigh faded.

In Figure 6.5, it can be observed that at fixed density of MUEs and threshold value, as the density of FAPs increases, the average coverage probability of the FUE also increases. This increment is due to the fact that as the density of FAPs increases in a fixed region, the probability of FAP to get closer to the FUE also increases, which in turn provide the higher SIR to the FUE. Moreover, it can also be observed that for 1000 FAPs, the average coverage probability is approximately 72%. This upper bound is due to the

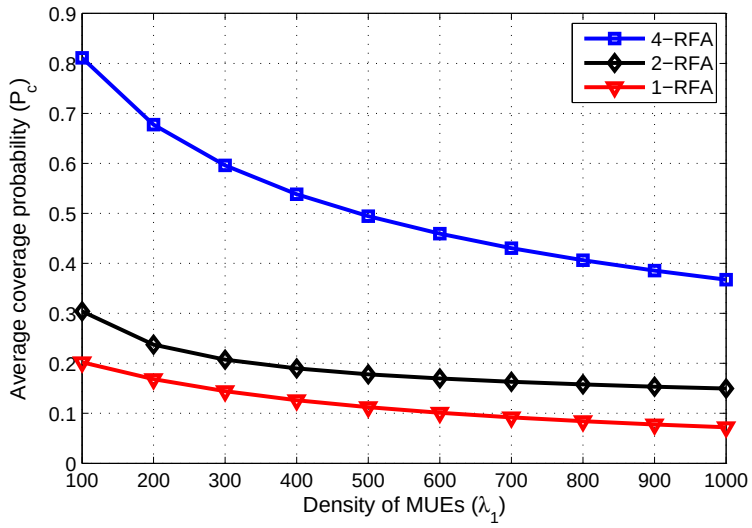

Figure 6.6: Average coverage probability of FUE at different density of MUEs (λ_1); ($\lambda_2 = 1600, \tau = -6.98dB$)

tighter selection of threshold. For lower values of threshold, i.e., $-10dB$, the average coverage probability nearly approaches to 1. It can also be seen that 4-RFA provides the highest coverage probability for FUE as compared to the other RFA schemes. This is because in case of 4-RFA, the cross-tier interference from uplink MUEs in the distant region is very small due to the large path loss between them as compared to the other RFA schemes, i.e., R_1-FUE receives cross-tier interference from the uplink MUEs in the distant region R_3. Moreover, in 4-RFA, the regions become smaller as compared to the 1 and 2-RFA, which increases the probability of FAPs to get closer to FUE and reduce the number of interferers in each region.

In Figure 6.6, it can be seen that at fixed density of FAPs and threshold value, as the density of MUEs increases, the average coverage probability of the FUE decreases. This decrement is due to the fact that the density of up-

link MUEs (interferers) increases in each region which in turn increases the cross-tier interference. In case of 4-RFA, the decrement in average coverage probability is much lower as compared to the other RFA schemes. The reason is that the 4-RFA divides the entire cell in such a way that the each region has less number of interferers as compared to 1 and 2-RFA. For example, if the density of MUEs is 100 in the entire cell, each region of 2-RFA consists of 50 uplink MUEs while each region of 4-RFA consists of 25 uplink MUEs on the average. In 1-RFA, all MUEs are deployed in a single region. Therefore, 4-RFA outperforms the other RFA schemes by assigning less number of interferers in each region.

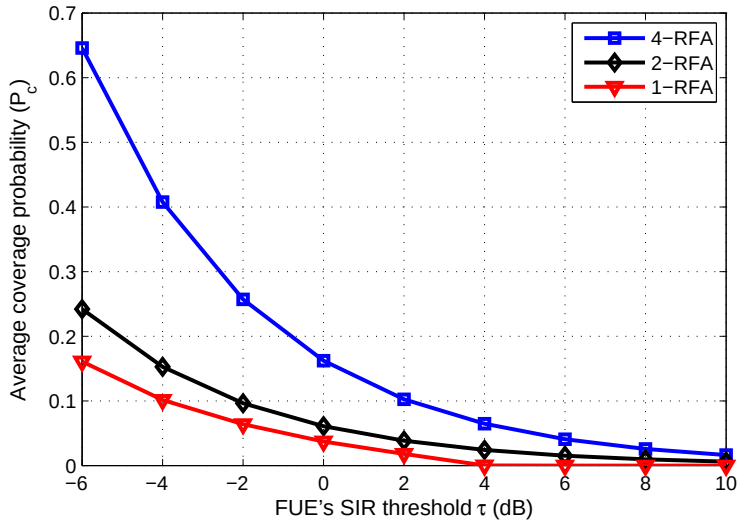

Figure 6.7: Average coverage probability of FUE at different SIR threshold (τ); ($\lambda_1 = 200, \lambda_2 = 1600$)

Figure 6.7 shows the coverage probability of an FUE for different values of threshold at fixed densities of MUEs and FAPs. It can be noticed that for lower values of threshold, 4-RFA outperforms the other RFA schemes. The

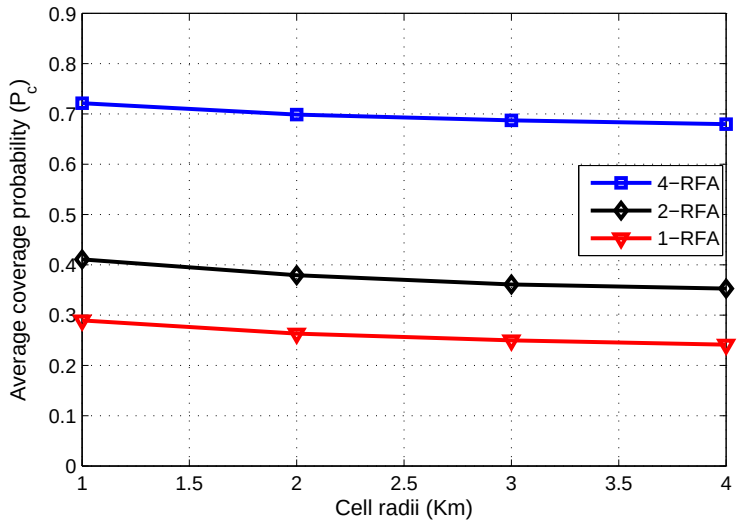

Figure 6.8: Average coverage probability of FUE at different cell radius; $(\lambda_1 = 200, \lambda_2 = 1600, \tau = -6.98dB)$

reason is that 4-RFA provides the higher coverage to an FUE because of the reason mentioned earlier. Moreover, in 4-RFA, the regions become smaller as compared to 1 and 2-RFA, which increases the probability of FAPs of getting closer to the FUE. As a result the SIR of FUE in each region becomes greater than the pre-defined threshold.

Figure 6.8 shows the coverage probability of an FUE at different cell radius for different RFA schemes. The densities of MUEs(λ_1), FAPs(λ_2) and threshold (τ) value is kept constant. It can be seen that as the radius of the macrocell increases, the coverage probability of FUE almost remains constant for different RFA schemes. This is because when the macrocell radius increases, the path loss between an FUE and the interferers increases. At the same time, the path loss between that FUE and the desired FAP also increases. Therefore, the average coverage probability of the FUE remains

same over all the macrocell radii. It can also be observed that the 4-RFA outperforms the other RFA schemes for all macrocell radii due to the aforementioned reasons.

Chapter 7

Conclusion and Future Work

7.1 Conclusion

Dense deployment of femtocells provides high data rates to the indoor users. It also enables the network operators to offload the traffic from macro base station. In order to achieve a good QoS and coverage, co-tier and cross-tier interferences are the major problems among femto-femto and femto-macro networks, respectively. The reverse frequency allocation scheme is one of the robust techniques in term of interference mitigation and spectral efficiency, particularly in downlink traffic. We have proposed an RFA scheme in the downlink by dividing the cell into multiple regions. Specifically, we studied the 4 region and 2 region RFA schemes. The simulation results show that the 4-region RFA with optimal cell radii provides a reduced average system outage probability as compared to the 2-region RFA in terms of a certain number of users and femtocells. Moreover, by increasing the cell radius, 4-region RFA outperforms the 2-region RFA in term of system outage for certain values of path loss exponent. Moreover, We have provided a multiple

region 2-tier downlink model using reverse frequency allocation scheme. The analytical model consists of two independent tiers of MUEs and FAPs that are modeled as independent PPPs. We have derived a closed-form expression of the coverage probability of an FUE using various forms of RFA algorithm under open access mode. The simulation results shows that 4-RFA outperforms the other RFA schemes at different densities of FAPs and MUEs as well as for different values of threshold without distrubing the spectral efficiency of the network.

7.2 Future Work

The overall analysis of RFA for a general user, whether FUE or MUE, with higher multiple regions and multiple cell scenarios is left as a future work. Also in this work, macrocell region is divided into equal circular areas, however, an optimization problem can be formulated where the region's radii are found optimally to provide better performance. Moreover, with the RFA approach, a FUE receives interference from other MUEs instead of from MBS, as it uses to be the case in classical systems. The same for BSs, that receive interference from other BSs instead of from other UEs. However, the propagation model for a UE to UE link is in general different from the propagation model for a BS to UE link, since both transmitter and receiver are located at low heights, and more obstacles can appear. The same occurs for a BS to BS propagation model where in this case situations of line of sight (and thus of high interference) may arise. This may lead to the use of different propagation coefficients in co-tier and cross-tier interferences. Also this work can be extended by including shadowing in the proposed model.

Bibliography

[1] M. Reardon, "Cisco predicts wireless data explosion", Press release, 9th Feb 2010, online available.

[2] D. L. Perez, G. D. la Roche, A. Valcarce, A. Juttner, and J. Zhang, "Interference avoidance and dynamic frequency palnning for WiMAX femtocells networks", *11th IEEE Singapore Intl. Conf. on Commun.,* pp. 1579-1584, 19-21 Nov. 2008.

[3] V. Chandrasekhar, J. G. Andrews and A. Gatherer, "Femtocell networks: a survey", *IEEE Commun. Mag.,* vol. 46, no. 9, pp. 59-67, Sep. 2008.

[4] Presentations by ABI Research, Picochip, Airvana, IP access, Gartner, Telefonica Espana, "Home access points and femtocells", *2nd Intl. Conf.* Available: http://www.avrenevents.com/dallasfemto2007/purchase presentations. html

[5] J. Cullen, "Radioframe presentation", in Femtocell Europe, London, UK, June. 2008.

[6] M. Yavuz, F. Meshkati, S. Nanda, A. Pokhariyal, N. Johnson, B. Roghothaman, and A. Richardson, "Interference management and per-

formance analysis of umts/hspa+ Femtocells", *IEEE Commun. Mag.,* vol. 47, no. 9, pp. 102-109, Sep. 2009.

[7] J. Zhang and J. G. Andrews, "Distributed antenna system with randomness", *IEEE Trans. Wireless Commun.,* vol. 7, no. 9, pp. 3636-3646, Sep. 2008.

[8] T. Wirth, L. Thiele, T. Haustein, O. Braz, and J. Stefanik, "LTE amplify and forward relaying for indoor coverage extension", *IEEE 72nd Vehicular Technology Conf. Fall*, vol. 147, pp. 1-5, Oct. 2010.

[9] V. Venkatkumar, T. Wirth, T. Haustein, and E. Schulz, "Relaying in long term evolution: Indoor full frequency reuse", *European Wireless (EW)*, vol. 149, pp. 298-302, May. 2009.

[10] T. Wirth, V. Venkatkumar, T. Haustein, E. Schulz, and R. Halfmann, "LTE-advanced relaying for outdoor range extension", *IEEE Vehicular Technology Conf. Fall, Anchorage, USA*, pp. 1-4, Sep. 2009.

[11] H. Claussen, "Performance of macro and co channel femtocells in a hierarchical cell structure", *IEEE 18th Intl. Symposium on Personal, Indoor and Mobile Radio Commun.,* pp. 1-5, 3-7 Sep. 2007.

[12] L. T. W. Ho and H. Claussen, "Effects of user-deployed, co-channel femtocells on the call drop probability in a residential scenario", *IEEE 18th Intl. Symposium on Personal, Indoor and Mobile Radio Commun.,* pp. 1-5, 3-7 Sep. 2007.

[13] R. Baines, "The need for WiMAX picocell and femtocells", WiMax, London, pp. 1-36, 25-26, Apr. 2007.

[14] T. Zahir, K. Arshad, A. Nakata, K. Moessner, "Interference management in femtocells," *Commun. Surveys Tutorials, IEEE*, vol. 15, no. 1, pp. 293-311, First Quarter 2013.

[15] S. F. Hasan, N. H. Siddique, and S. Chakraborty, "Femtocell versus Wi Fi- A survey and comparison of architecture and performance", *1st Intl. Conf. on Wireless Commun., Vehicular Technology, Information Theory and Aerospace and Electronic Systems Technology*, pp. 916-920, 17-20 May. 2009.

[16] J. O. Carroll, H. Claussen, and L. Doyle, "Partial GSM spectrum reuse for femtocells", *IEEE 20th Intl. Symposium on Personal, Indoor and Mobile Radio Commun.,* pp. 2111-2116, 13-16 Sep. 2009.

[17] S. S. Prasad and R. Baruah, "Femtocell mass deployment: India perspective", *3rd Intl. Conf. on Anti-counterfeiting, Security, and Identification in Commun.,* pp. 34-37, 20-22 Aug. 2009.

[18] D. Knisely, T. Yoshizawa, and F. Favichia, "Standardization of femtocells in 3GPP", *IEEE Commun. Mag.,* vol. 47, no. 9, pp. 68-75, Sep. 2009.

[19] D. Choi et.al, "Dealing with loud neighbours: The beneïňĄts and tradeoffs of adaptive femtocell access", *IEEE Globcomm.,* Dec. 2012.

[20] D. Das and V. Ramaswamy, "Co-channel femtocell-macrocell deployments-access control", *IEEE 70th Vehicular Technology Conference Fall*, pp. 1-6, 20-23 Sep. 2009.

[21] A. Valcarce, D. Lopez-Perez, G. D. L. Roche, and Z. Jie, "Limited access to ofdma femtocells", *IEEE 20th Intl. Symposium on Personal, Indoor and Mobile Radio Commun.,* pp. 1-5, 13-16 Sep. 2009.

[22] L. Wang, Z. Yongsheng, and W. Zhenrong, "Mobility management schemes at radio network layer for lte femtocells", *IEEE 69th Vehicular Technology Conf.,* pp. 1-5, 26-29 Apr. 2009.

[23] H. Su, L. Kuang, and J. Lu, "Interference avoidance in OFDMA based femtocell network", *IEEE Youth Conf. on Information Computing and Telecomm.,* pp. 126-129, 20-21 Sep. 2009.

[24] A. Golaup, M. Mustapha, and L. B. Patanapongipibul, "Femtocell access control strategy in umts and lte", *IEEE Commun. Mag.,* vol. 47, no. 9, pp. 117-123, Sep. 2009.

[25] J. Zhang, de la Roche, E. Liu, "Introduction in Femtocells: Technologies and Deployment", John Wiley Sons, Ltd, Chichester, UK, 2009.

[26] S.P. Yeh, S. Talwar, S.-C. Lee, and H. Kim, "WiMAX femtocells: A perspective on network architecture, capacity, and coverage", *IEEE Commun. Mag.,* vol. 46, no. 10, pp. 58-65, Oct. 2008.

[27] D. Lpez-Prez, A. Valcarce, G. de la Roche, and J. Zhang, "OFDMA femtocells: A roadmap on interference avoidance", *IEEE Commun. Mag.*, vol. 47, no. 9, pp. 41-48, Sep. 2009.

[28] K. Cho, W. Lee, D. Yoon, K. Hyun, Yun-Sung Choi, "Resource alloation for orthogonal and co-channel femtocells in a hierarchical cell structure",

IEEE 13th Intl. Symposium on Consumer Electron (ISCE), pp. 655-656, May. 2009.

[29] P. Lee, T. Lee, J. Jeong, J. Shin, "Interference management in LTE femtocell systems using fractional frequency reuse", *12th Intl. Conf. on Adv. Commun. Tech.: ICT for Green Growth and Sustainable Development (ICACT)*, vol. 2, pp. 1047-1051, Feb. 2010.

[30] N. Saquib, E. Hossain, D. I. Kim, "Fractional frequency reuse for interference management in LTE-advanced hetnets," *Commun. Surveys Tutorials, IEEE*, vol. 20, no. 2, pp. 113-122, April, 2013.

[31] T. Zahir, K. Arshad, Y. Ko, and K. Moessner, "A downlink power control scheme for interference avoidance in femtocells," *7th Intl. Wireless Commun. and Mobile Computing Conf. (IWCMC)*, pp. 1222-1226, 4-8 July, 2011.

[32] M. Z. Chowdhury, Y. M. Jang, Z. J. Haas, "Interference mitigation using dynamic frequency reuse for dense femtocell network architectures", *2nd Intl. Conf. on Ubiquitous and Future Net. (ICUFN)*, pp. 256-261, 16-18 June. 2010.

[33] M. Z. Chowdhury, Y. M. Jang, Z. J. Haas, "Cost-effective frequency planning for capacity enhancement of femtocellular networks", *Wireless Personal Commun.,* vol. 60, Issue 1, pp. 83-104, Sep. 2011.

[34] P. Jacob, A. James, A. S. Madhukumar, "Downlink interference Reduction through Reverse Frequency Allocation", *Intl. Conf. on Commun. Systems (ICCS)*, pp. 329-333, 21-23 Nov. 2012.

[35] H. S. Dhillon, R. K. Ganti, F. Baccelli and J. G. Andrews, "Modeling and Analysis of K-Tier Downlink Heterogeneous Cellular Networks", *IEEE Journal on Sel. Areas in Commun.,* vol. 30, no. 3, pp. 550-560, Apr. 2012.

[36] S. Catreux, P. F. Driessen, and L. J. Greenstein, "Simulation results for an interference-limited multiple-input multiple-output cellular system", *IEEE Commun. Lett.,* vol. 4, no. 11, pp. 334-336, Nov. 2000.

[37] T. X. Brown, "Cellular performance bounds via shotgun cellular systems", *IEEE J. Sel. Areas Commun.,* vol. 18, no. 11, pp. 2443-2455, Nov. 2000.

[38] F. Baccelli, M. Klein, M. Lebourges, and S. Zuyev, "Stochastic geometry and architecture of communication networks", *J. Telecomm. Systems,* 1997.

[39] F. Baccelli and S. Zuyev, "Stochastic geometry models of mobile communication networks", *in Frontiers in Queueing. Boca Raton, FL: CRC Press,* pp. 227-243, 1997.

[40] J. G. Andrews, F. Baccelli, and R. K. Ganti, "A tractable approach to coverage and rate in cellular networks", *IEEE Trans. Commun.,* vol. 59, no. 11, pp. 3122-3134, Nov. 2011.

[41] D. Stoyan, W. Kendall, and J. Mecke, "Stochastic Geometry and Its Applications", 2nd ed. John Wiley and Sons, 1996.

[42] F. Baccelli and B. Blaszczyszyn, "Stochastic Geometry and Wireless Networks", Now: Foundations and Trends in Networking, 2010.

[43] S. Mukherjee, "Analysis of UE outage probability and macrocellular traffic offloading for WCDMA macro network with femto overlay under closed and open access", *in Proc., IEEE Intl. Conf. on Commun.,* Kyoto, Japan, June. 2011.